

# Current fluctuations in a semi-infinite line

Soumyabrata Saha<sup>1</sup> and Tridib Sadhu<sup>2</sup>

Department of Theoretical Physics, Tata Institute of Fundamental Research, Homi Bhabha Road, Mumbai 400005, India

E-mail: <sup>1</sup>soumyabrata.saha@tifr.res.in and <sup>2</sup>tridib@theory.tifr.res.in

**Abstract.** We present an application of a fluctuating hydrodynamic theory to study current fluctuations in diffusive systems on a *semi-infinite* line in contact with a reservoir with a *slow* coupling. Within this hydrodynamic framework, we show that the distribution of time-integrated current across the boundary at large times follows a large deviation principle with a rate function that depends on the coupling strength with the reservoir. The system exhibits a long-term memory of its initial state which was earlier reported on an infinite line and can be described using quenched and annealed averaging on the initial state. We present an explicit expression of the rate function for independent particles, which we verify using an exact solution of the microscopic dynamics. For the symmetric exclusion process we present expression of the first three cumulants for both quenched and annealed ensemble.

*Keywords:* Exclusion process, Large deviations, Fluctuating hydrodynamics, Slow bond, Macroscopic fluctuation theory.

## 1. Introduction

Non-equilibrium processes are ubiquitous in nature. However, unlike equilibrium statistical mechanics, no universal framework exists to study macroscopic fluctuations for out-of-equilibrium systems. In the past two decades a powerful hydrodynamic theory, commonly referred as the macroscopic fluctuation theory (MFT), has emerged [1, 2] that presents a systematic approach for studying fluctuations in diffusive transport models. Since its inception in early 2000 by Bertini, De Sole, Gabrielli, Jona-Lassinio, and Landim [3, 4] the theory has been successfully applied in a varied range of non-equilibrium scenarios. Notably, the exact results for the large deviations of density [5] and current [6, 7] in the non-equilibrium stationary state of the symmetric exclusion process on a finite line have been independently reproduced [4, 8–10] within this hydrodynamic approach. On an infinite line, the highly non-trivial Bethe ansatz result [11] about current fluctuations in the symmetric simple exclusion process has been recently reproduced [12] using the MFT formalism [13] by discovering a remarkable connection with an integrable model. Similar exact results about large deviations in related transport models [14], tracer statistics in single-file [15, 16], height fluctuations in KPZ [17, 18] have made the MFT a reliable theoretical approach.

For the exclusion process the two commonly studied geometry in the literature are finite one dimensional lattice coupled with two unequal reservoirs at the boundary and infinite lattice starting with a non-stationary state. The two geometry represents two different non-equilibrium scenarios. A finite system reaches a non-equilibrium stationary state driven by the unequal particle reservoirs at the two ends where the initial state of the system becomes irrelevant. On the other hand an infinite system started with a step initial density profile takes infinite time to reach the asymptotic equilibrium state. For the latter, it was found that the initial state plays a determining factor in the fluctuations even at large times.

In this paper, our interest is in the intermediate geometry: a semi-infinite system coupled with a reservoir at one end. When the initial density of the system is different from the reservoir density, the system is out of equilibrium and evolves to reach the asymptotic stationary state in equilibrium with the reservoir. Studies of this geometry are significantly scarce. Earliest work about exclusion process on semi-infinite lattice is by Liggett [19] and then by Grosskinsky [20]. For the asymmetric exclusion process, Sassamoto and Williams showed [21] that there is a convergence to a local stationary state where spatial correlation of density has an exact correspondence with the correlation in the finite geometry. Recently Duhart et al [22] derived the large deviations function for the empirical density in the local stationary state. There is an exact result [23] about transition probability that has been exploited to obtain the mean and the variance of integrated current for the symmetric exclusion process for an initial state with Bernoulli measure. These exact results about the two cumulants are related to the cumulants of current on an infinite line coupled to a reservoir at the centre [24].

A reason for us working with the semi-infinite geometry is that the effect of reservoir

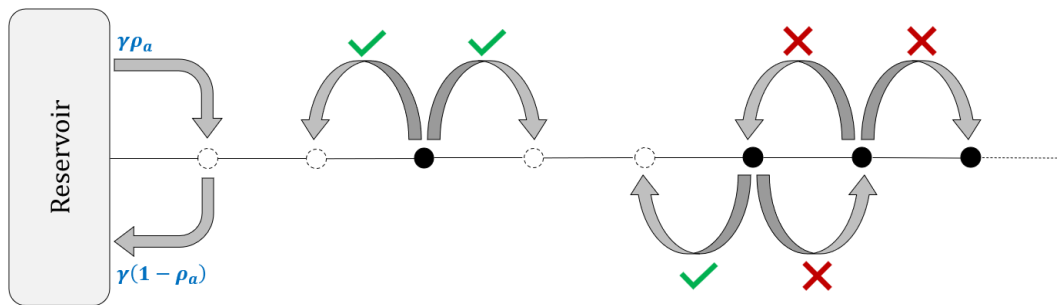


**Figure 1.** The symmetric simple exclusion process on a one dimensional semi-infinite lattice coupled with the boundary reservoir of density  $\rho_a$ , where  $\gamma$  represents the strength of the jump rates. In the bulk, jump rates are of unit strength.

on the boundary layer can be studied for the non-stationary state. At the same time we are able to study how the system keeps a long-term memory of its initial state in presence of the reservoir.

In order to understand the effect of the reservoir we introduce a tuning parameter  $\gamma > 0$  for the jump rates to and from the reservoir. A large  $\gamma \gg 1$  implies a fast time scale at the boundary compared to the bulk dynamics and one would expect the latter to be the determining factor for transport. For small  $\gamma \ll 1$ , the slow boundary rates are the bottleneck. The question we ask is how different are the fluctuations in these two regimes and whether there is a scale of  $\gamma$  that demarcates the two regimes.

For a quantitative answer, we consider two simple examples: particles hopping on a semi-infinite  $\mathbb{Z}^+$  lattice (a) without an inter-particle interaction (b) and with onsite exclusion interactions. The second example is known as the symmetric simple exclusion process (SSEP) whose dynamics is sketched in figure 1. The jump rates at the boundary correspond to a reservoir of density  $\rho_a$  independent of the parameter  $\gamma$  which only controls the time-scale compared to the bulk dynamics. The low-density limit of SSEP corresponds to the first example of non-interacting particles.

We specifically look at the large time statistics of the time-integrated current  $Q_T$  across the system-reservoir boundary which gives the net influx of particles in total time  $T$  from the reservoir to the system. For a diffusive system like the two examples in consideration, the relevant scale for  $Q_T$  is  $\sim \sqrt{T}$ . We show that  $\gamma \sim T^{-1/2}$  is the marginal scale of the boundary rates that separates the slow and the fast coupling regimes. More accurately, for  $\gamma \sim T^\beta$  with  $\beta < 1/2$  the long time fluctuations of  $Q_T$  are independent of  $\gamma$  and are same as for the infinitely fast reservoir coupling. Similar behaviour was noted in [24] for SEP on a different geometry. In the slow coupling regime of  $\beta > 1/2$  the fluctuations are equilibrium-like. This behaviour is illustrated in figure 2.

Our understanding of this scenario is based on our analysis for  $\gamma = \frac{\Gamma}{\sqrt{T}}$ , where we show that the probability of  $Q_T$  follows a large deviation principle

$$\mathrm{P} \left( j = \frac{Q_T}{\sqrt{T}} \right) \asymp e^{-\sqrt{T}\phi(j)} \quad (1)$$

where  $\phi(j)$  is the large deviation function (ldf) of current. Here, the symbol  $\asymp$  implies

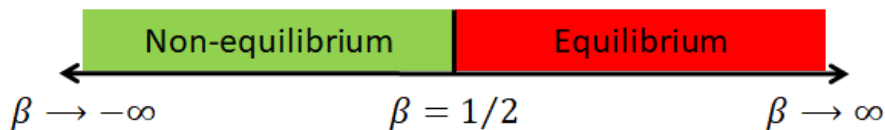


**Figure 2.** For the SSEP in figure 1 with  $\gamma \sim T^{-\beta}$ , the marginal value  $\beta = 1/2$  separates the equilibrium-like slow coupling regime and the non-equilibrium fast-coupling regime of the current fluctuations.

that the ratio of logarithm of two sides in (1) converges to 1 for large  $T$ . The ldf for  $\Gamma \rightarrow \infty$  characterises the fast coupling regime. The  $\Gamma \rightarrow 0$  gives the slow coupling regime where  $\phi(j)$  vanishes.

Infinite one dimensional systems are known to exhibit a long-term memory of initial state and our system is not an exception. To emphasize this dependence mostly two kinds of initial states are considered. In one, the initial state is drawn from an equilibrium measure where atypical fluctuations in the initial state contribute to the current fluctuations. In the second, only typical configurations in the initial state are allowed. The long-time statistics of  $Q_T$  or equivalently the ldf  $\phi(j)$  is different in the two ensembles of initial states. Drawing analogy with disorder averages in spin-glass, these two ensembles are referred as the annealed and quenched initial states, respectively. The analogy is more evident for the cumulant generating function (cgf) in the two ensembles

$$\mu_{\mathcal{A}}(\lambda) = \log \left( \langle \langle e^{\lambda Q_T} \rangle_{\text{hist.}} \rangle_{\text{init.}} \right) \quad \text{and} \quad \mu_{\mathcal{Q}}(\lambda) = \langle \log \left( \langle e^{\lambda Q_T} \rangle_{\text{hist.}} \right) \rangle_{\text{init.}} \quad (2)$$

where the subscripts ( $\mathcal{A}$  and  $\mathcal{Q}$ ) denote the respective ensembles, the  $\langle \rangle_{\text{hist}}$  denotes average over evolution, and  $\langle \rangle_{\text{init}}$  denotes average over the initial state. For  $\mu_{\mathcal{Q}}(\lambda)$  the initial-average of the slow-varying logarithm is dominated by the contribution from the most-typical configuration of the initial state. In the two examples we consider, the typical density profile in the initial state is chosen to be uniform density  $\rho_0(x) = \rho_b$ .

The essential physics can be seen already in the simplest example of the non-interacting particles. For the annealed ensemble

$$\lim_{T \rightarrow \infty} \frac{\mu_{\mathcal{A}}(\lambda)}{\sqrt{T}} = [\rho_a (e^\lambda - 1) + \rho_b (e^{-\lambda} - 1)] \Omega_\Gamma \quad (3a)$$

where the  $\Gamma$  dependence is in  $\Omega_\Gamma$  given by

$$\Omega_\Gamma = \frac{2}{\sqrt{\pi}} - \frac{1 - e^{\Gamma^2} \text{erfc } \Gamma}{\Gamma}. \quad (3b)$$

The expression is similar to the cgf of current on an infinite line [13] and on a finite lattice coupled with two reservoirs [25], with the difference in the overall factor  $\Omega_\Gamma$ .

For the quenched ensemble

$$\lim_{T \rightarrow \infty} \frac{\mu_{\mathcal{Q}}(\lambda)}{\sqrt{T}} = \rho_a (e^\lambda - 1) \Omega_\Gamma + \rho_b \int_0^\infty dx \log [1 + (e^{-\lambda} - 1) W_\Gamma(x)] \quad (4a)$$

where

$$W_\Gamma(x) = 1 - \frac{2\Gamma}{\pi} \int_0^\infty dz \frac{e^{-\pi^2 z^2}}{z(\Gamma^2 + \pi^2 z^2)} (\Gamma \sin \pi x z + \pi z \cos \pi x z). \quad (4b)$$

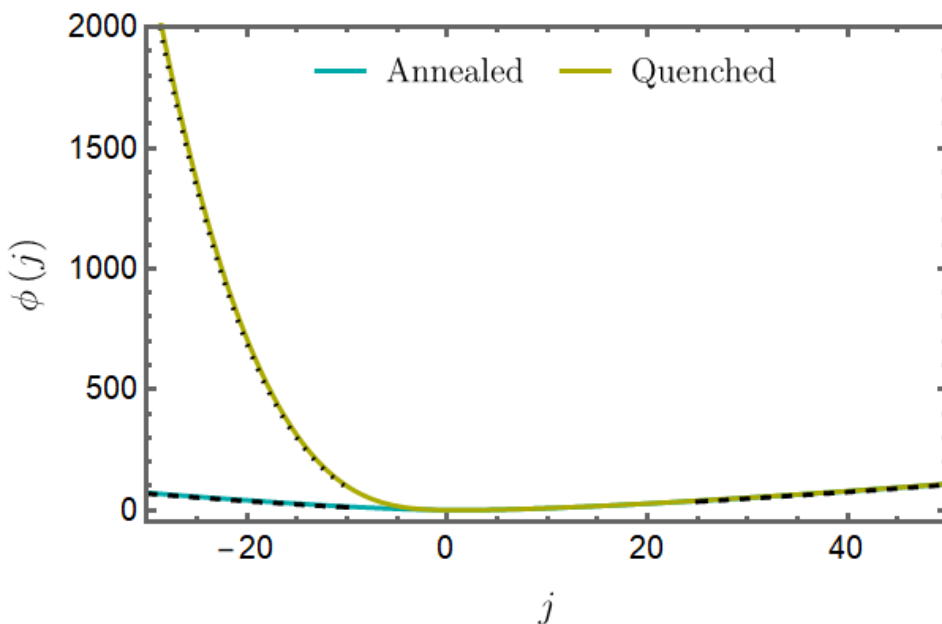


**Figure 3.** A comparison between the annealed and the quenched large deviation functions for the fast coupling limit ( $\Gamma \rightarrow \infty$ ). The dashed lines indicate a  $j \log j - j$  asymptotic whereas the dotted line indicates  $j^3$  growth.

It is instructive to compare similar result on the infinite line [13].

The long-time scaling of the cgf implies the large deviation asymptotics in (1) where the ldf  $\phi(j)$  is related to the cgf by a Legendre-Fenchel transformation

$$\mu(\lambda) \simeq \sqrt{T} \max_j (j\lambda - \phi(j)). \quad (5)$$

The ldf for the two ensembles for the fast coupling regime is shown in figure 3. For large positive  $j$ , the ldf for both ensembles grow as  $j \log \frac{j}{\rho_a \Omega_\Gamma} - j$ . For large negative  $j$ , the ldf for annealed ensemble grows as  $|j| \log \frac{|j|}{\rho_b \Omega_\Gamma} - |j|$  whereas for the quenched it has steeper growth  $\frac{|j|^3}{12\rho_b^2}$ . The positive tail of the quenched ldf is different for the infinite line [13].

For the SSEP our results are limited and we have expressions for only up to the third cumulant. The average of  $Q_T$  is same for the two ensembles and is given by

$$\frac{\langle Q_T \rangle}{\sqrt{T}} \simeq (\rho_a - \rho_b) \Omega_\Gamma \quad (6)$$

For the fast coupling limit  $\Omega_\Gamma \simeq 2/\sqrt{\pi}$  and the resulting expression (6) is consistent with the exact result in [23].

The difference between the two ensembles emerge at the second and higher cumulants. Their expression is simpler in the fast coupling regime which we present below. For annealed, the variance

$$\frac{\langle Q_T^2 \rangle_A}{\sqrt{T}} \simeq \frac{1}{\sqrt{\pi}} \left[ 2(\rho_a + \rho_b) - 4(\sqrt{2} - 1)(\rho_a^2 + \rho_b^2) - 4(3 - 2\sqrt{2})\rho_a\rho_b \right] \quad (7)$$

whereas the variance for the quenched ensemble differs from the annealed

$$\frac{\langle Q_T^2 \rangle_Q}{\sqrt{T}} \simeq \frac{\langle Q_T^2 \rangle_A}{\sqrt{T}} - \frac{1}{\sqrt{\pi}} \left[ 2(2 - \sqrt{2})\rho_b(1 - \rho_b) \right]. \quad (8)$$

The expression (7) for the annealed ensemble is consistent with an earlier result [24] for  $\rho_a = 1$  and  $\rho_b = 0$ .

The third cumulant for the annealed is

$$\frac{\langle Q_T^3 \rangle_A}{\sqrt{T}} \simeq \frac{(\rho_a - \rho_b)}{\sqrt{\pi}} \left[ 2 - \frac{8}{3} \left( 9\sqrt{2} - 8\sqrt{3} \right) (\rho_a - \rho_b)^2 + 12 \left( 1 - \sqrt{2} \right) (\rho_a + \rho_b - 2\rho_a\rho_b) \right] \quad (9)$$

For the quenched we have an explicit result only for density  $\rho_b = 0$ , where it is equal to the annealed result (9).

Our results for the two models are obtained using the hydrodynamic formalism of the MFT for the semi-infinite geometry with slow boundary. In recent years there is increasing interest in understanding the effect of slow coupling for the hydrodynamic description. To our knowledge, the earliest study in this direction was in [26] for finite SSEP coupled with two reservoirs. The work established that the average macroscopic density profile in the steady state is a solution of the heat equation with Dirichlet, Robin, or Neumann boundary conditions, depending on the speed of the rates at the boundary. The work was later extended in [27–33], particularly for small fluctuations in the steady state. Variants of the model with slow rates have also been studied in [34–40].

For an hydrodynamic approach to study fluctuations of  $Q_T$  at large  $T$ , we define re-scaled coordinates  $(x, t) := (\frac{i}{\sqrt{T}}, \frac{\tau}{T})$  where  $i = 1, 2, \dots$  is the site index of the semi-infinite lattice and  $\tau$  is the microscopic time. We show that the average density  $\rho_{\text{av}}(\frac{i}{\sqrt{T}}, \frac{\tau}{T}) \simeq \langle n_i(\tau) \rangle$  for large  $T$ , where  $n_i(\tau)$  denotes the occupation of the  $i$ -th site at time  $\tau$ , follows the heat equation

$$\frac{\partial \rho_{\text{av.}}(x, t)}{\partial t} = \frac{\partial^2 \rho_{\text{av.}}(x, t)}{\partial x^2} \quad (10a)$$

with a Robin boundary condition

$$\rho_{\text{av.}}(x, t) - \frac{1}{\Gamma} \frac{\partial \rho_{\text{av.}}(x, t)}{\partial x} = \rho_a \quad \text{at } x = 0. \quad (10b)$$

This is in agreement with rigorous mathematical results of [26–30].

The density  $\rho(\frac{i}{\sqrt{T}}, \frac{\tau}{T}) \simeq n_i(\tau)$  for large  $T$  fluctuates around the average  $\rho_{\text{av}}(x, t)$ . For SSEP, we argue that it satisfies a fluctuating hydrodynamics equation

$$\frac{\partial \rho(x, t)}{\partial t} = \begin{cases} -\frac{\partial \rho(x, t)}{\partial x} + \xi(t) & \text{for } x = 0 \\ \frac{\partial^2 \rho(x, t)}{\partial x^2} + \frac{\partial \eta(x, t)}{\partial x} & \text{for } x > 0 \end{cases} \quad (11a)$$

where  $\eta(x, t)$  is a weak Gaussian white noise with zero mean and covariance

$$\langle \eta(x, t) \eta(x', t') \rangle = \frac{1}{\sqrt{T}} 2\rho(x, t)(1 - \rho(x, t)) \delta(x - x') \delta(t - t') \quad (11b)$$

and  $\xi(t)$  is a noise delta correlated in time with a moment generating function

$$\langle e^{h\xi(t)} \rangle = e^{H_{\text{bdry}}[\rho(0, t), h]} \quad (11c)$$

with

$$H_{\text{bdry}}[\rho, h] = \Gamma [\rho_a (1 - \rho) (e^h - 1) + \rho (1 - \rho_a) (e^{-h} - 1)]. \quad (11d)$$

(The reason for the subscript “bdry” will be evident in the next section 2.) Our argument for (11a) is based on an Action formulation of the microscopic dynamics and an uncontrolled gradient expansion to obtain the hydrodynamic limit.

We apply the MFT formulation for (11a) which gives the cgf of  $Q_T$  as the solution of a variational problem. We explicitly solve the latter in the low density limit which corresponds to the non-interacting particles. The result is then verified using an exact solution of the microscopic dynamics. For arbitrary density, a perturbation solution of the variational problem gives our result for the first few cumulants of  $Q_T$ .

The rest of this article is organized as follows. In Section 2, we present the variational formalism for the cgf of  $Q_T$ . In Section 3 we solve the variational problem for the non-interacting particles and the solution is verified using microscopic dynamics in Section 4. Section 5 presents a perturbation solution of the variational problem for SSEP. We conclude with open directions in Section 6. In the Appendix A we present an argument for (11a) and in Appendix D we present a derivation for (10a, 10b).

## 2. A fluctuating hydrodynamic approach for current fluctuations

We recall the variational formulation of MFT [1,2,41] for current fluctuation in the SSEP on the semi-infinite line with slow coupling to reservoir. For large  $T$ , the time-integrated current across the system-reservoir boundary relates to the density

$$Q_T = \sqrt{T} \int_0^\infty dx (\rho(x, 1) - \rho(x, 0)) \quad (12)$$

which is a consequence of particle number conservation in the bulk. Within the MFT formulation the moment-generating function of  $Q_T$  is expressed as a path integral over the density field  $\rho(x, t)$  and a conjugate response field  $\hat{\rho}(x, t)$ .

$$\langle e^{\lambda Q_T} \rangle = \int \mathcal{D}[\rho, \hat{\rho}] e^{-\sqrt{T} S[\rho, \hat{\rho}]} \quad (13)$$

where the action

$$S[\rho, \hat{\rho}] = -\lambda \int_0^\infty dx (\rho(x, 1) - \rho(x, 0)) + \mathcal{F}[\rho(x, 0)] + \int_0^1 dt \left[ \int_0^\infty dx \left( \hat{\rho}(x, t) \frac{\partial \rho(x, t)}{\partial t} \right) - H[\rho, \hat{\rho}] \right] \quad (14)$$

with an effective Hamiltonian [1, 2, 41]

$$H[\rho, \hat{\rho}] = H_{\text{bdry}}[\rho(0, t), \hat{\rho}(0, t)] + \int_0^\infty dx \left( \frac{\sigma(\rho)}{2} \frac{\partial \hat{\rho}(x, t)}{\partial x} - D(\rho) \frac{\partial \rho(x, t)}{\partial x} \right) \frac{\partial \hat{\rho}(x, t)}{\partial x} \quad (15)$$

with the  $H_{\text{bdry}}$  defined in (11d) represents the contribution from the slow coupling with the boundary reservoir. For the SSEP, the diffusivity  $D(\rho) = 1$  and the mobility  $\sigma(\rho) = 2\rho(1 - \rho)$ . We use the functions  $D$  and  $\sigma$  instead of their explicit expression to make the discussions easily generalizable to other models which differ in the transport coefficients and  $H_{\text{bdry}}$ . In Appendix A we give a simplistic non-rigorous derivation of the

action for the semi-infinite line. The expression (14) for  $\lambda = 0$  and  $\mathcal{F} = 0$  is the Martin-Siggia-Rose-Janssen-de-Dominicis action [42, 43] for the fluctuating hydrodynamics equation (11a) where  $\hat{\rho}$  is the response field.

The term  $\mathcal{F}$  in (14) is the contribution from the initial state, which for the annealed ensemble is the ldf of the density  $\rho(x, 0)$  in the initial equilibrium state of uniform average profile  $\rho_b$ . For the semi-infinite line its explicit expression is [44]

$$\mathcal{F}[\rho(x, 0)] = \int_0^\infty dx \int_{\rho_b}^{\rho(x, 0)} dr \frac{2D(r)}{\sigma(r)} (\rho(x, 0) - r) \quad (16)$$

For the quenched ensemble the leading contribution comes from  $\rho(x, 0) = \rho_b$  for which  $\mathcal{F} = 0$  in the action (14).

For large  $T$ , the path-integral in (13) is dominated by the least-action path and

$$\mu(\lambda) \simeq -\sqrt{T} \min_{\rho, \hat{\rho}} S[\rho, \hat{\rho}] \quad (17)$$

We shall denote the least-action paths by  $(\rho, \hat{\rho}) \equiv (q, p)$ . The calculus of variations gives [13] the least-action paths as solutions of

$$\frac{\partial q(x, t)}{\partial t} = \frac{\partial}{\partial x} \left( D(q) \frac{\partial q(x, t)}{\partial x} \right) - \frac{\partial}{\partial x} \left( \sigma(q) \frac{\partial p(x, t)}{\partial x} \right) \quad \text{and} \quad (18a)$$

$$\frac{\partial p(x, t)}{\partial t} = -D(q) \frac{\partial^2 p(x, t)}{\partial x^2} - \frac{\sigma'(q)}{2} \left( \frac{\partial p(x, t)}{\partial x} \right)^2. \quad (18b)$$

with the contribution from the  $H_{\text{bdry}}$  term included in the spatial boundary condition at  $x = 0$  for all  $t$ :

$$D(q) \frac{\partial p}{\partial x} = -\frac{\delta H_{\text{bdry}}}{\delta q(0, t)} = \Gamma [\rho_a (e^{p(0, t)} - 1) - (1 - \rho_a) (e^{-p(0, t)} - 1)] \quad (19a)$$

$$\sigma(q) \frac{\partial p}{\partial x} - D(q) \frac{\partial q}{\partial x} = \frac{\delta H_{\text{bdry}}}{\delta p(0, t)} = \Gamma [\rho_a (1 - q(0, t)) e^{p(0, t)} - q(0, t) (1 - \rho_a) e^{-p(0, t)}]. \quad (19b)$$

The optimization also gives [13] the temporal boundary conditions, which differs in the two ensembles. For the annealed ensemble, they are given as

$$p(x, 0) = \lambda + \int_{\rho_b}^{q(x, 0)} dr \frac{2D(r)}{\sigma(r)} \quad \text{and} \quad p(x, 1) = \lambda. \quad (20)$$

For the quenched ensemble, the temporal boundary conditions are

$$q(x, 0) = \rho_b \quad \text{and} \quad p(x, 1) = \lambda. \quad (21)$$

For both ensembles, using the least-action path (18a) and the boundary condition (19b), the expression (14) for the minimal action (17) simplifies

$$\begin{aligned} \frac{\mu(\lambda)}{\sqrt{T}} &\simeq \lambda Q_T - \mathcal{F}[q(x, 0)] - \int_0^1 dt \int_0^\infty dx \frac{\sigma(q)}{2} \left( \frac{\partial p}{\partial x} \right)^2 \\ &\quad + \int_0^1 dt \left( H_{\text{bdry}} - p(0, t) \frac{\delta H_{\text{bdry}}}{\delta p(0, t)} \right) \end{aligned} \quad (22)$$

This expression for the cgf holds true for any diffusive system.



**Remark:** For  $\lambda = 0$ , the least-action-path is  $p(x, t) = 0$  and  $q(x, t) = \rho_{\text{av}}(x, t)$  which is the solution of diffusion equation (10a) with  $q(x, 0) = \rho_b$  and the Robin boundary condition (10b). The fast coupling limit  $\Gamma \rightarrow \infty$  gives the Dirichlet boundary conditions  $q(0, t) = \rho_a$  and  $p(0, t) = 0$ , which are often argued in the literature. The slow coupling limit  $\Gamma \rightarrow 0$  gives the Neumann boundary conditions  $\partial_x q(x, t) = 0 = \partial_x p(x, t)$  at  $x = 0$ .

**Remark:** There are obvious symmetries [13] evident from the action (14). For the annealed ensemble, reflection symmetry implies  $\mu_{\mathcal{A}}(\lambda|\rho_a, \rho_b) = \mu_{\mathcal{A}}(-\lambda|\rho_b, \rho_a)$  and particle-hole symmetry implies  $\mu_{\mathcal{A}}(\lambda|\rho_a, \rho_b) = \mu_{\mathcal{A}}(\lambda|1-\rho_a, 1-\rho_b)$ . There is an additional symmetry [13]

$$\mu_{\mathcal{A}}(\lambda) = \mu_{\mathcal{A}}(f'(\rho_b) - f'(\rho_a) - \lambda) \quad (23)$$

due to invariance under time-reversal. These symmetries do not apply for the quenched ensemble.

### 3. Variational solution for non-interacting particles

The variational problem for SSEP in (17) is hard to solve in general. It is simpler to solve the low-density limit, which amounts to setting  $D(q) = 1$  and  $\sigma(q) = 2q$  in (14) with

$$H_{\text{bdry}} [q(0, t), p(0, t)] = \Gamma [\rho_a (e^{p(0,t)} - 1) + q(0, t) (e^{-p(0,t)} - 1)] \quad (24)$$

The least-action paths are (18a, 18b) with  $D(q) = 1$  and  $\sigma(q) = 2q$  and the spatial boundary condition at  $x = 0$  becomes

$$\frac{\partial p(x, t)}{\partial x} = \Gamma (1 - e^{-p(0,t)}) \quad (25a)$$

$$2q(x, t) \frac{\partial p(x, t)}{\partial x} - \frac{\partial q(x, t)}{\partial x} = \Gamma (\rho_a e^{p(0,t)} - q(0, t) e^{-p(0,t)}) \quad (25b)$$

In order to simplify (22) for the non-interacting many particle system, we use the identity [13]

$$q \left( \frac{\partial p}{\partial x} \right)^2 = \frac{\partial}{\partial t} (qp) - \frac{\partial}{\partial x} \left( p \frac{\partial q}{\partial x} - 2qp \frac{\partial p}{\partial x} - q \frac{\partial p}{\partial x} \right) \quad (26)$$

Using (25a, 25b) on top of the above identity, the cgf for the annealed ensemble in (22) simplifies to

$$\lim_{T \rightarrow \infty} \frac{\mu_{\mathcal{A}}(\lambda)}{\sqrt{T}} = \Gamma \rho_a \int_0^1 dt (e^{p(0,t)} - 1) + \rho_b \int_0^\infty dx (e^{-\lambda} e^{p(x,0)} - 1), \quad (27)$$

while in the quenched ensemble, with  $\mathcal{F} = 0$  in (22), the simplified cgf looks like

$$\lim_{T \rightarrow \infty} \frac{\mu_{\mathcal{Q}}(\lambda)}{\sqrt{T}} = \Gamma \rho_a \int_0^1 dt (e^{p(0,t)} - 1) + \rho_b \int_0^\infty dx (p(x, 0) - \lambda). \quad (28)$$

The linearized least-action equations for this problem is simple to solve using a known [13] canonical transformation  $(G, R) := (e^p, qe^{-p})$ . The new variables  $G$  and  $R$  are decoupled and follows

$$\frac{\partial G(x, t)}{\partial t} = -\frac{\partial^2 G(x, t)}{\partial x^2} \quad \text{and} \quad \frac{\partial R(x, t)}{\partial t} = \frac{\partial^2 R(x, t)}{\partial x^2} \quad (29)$$

which are easy to solve using Greens function method. In terms of new variables, the temporal boundary condition (20) at final time  $t = 1$  gives

$$G(x, 1) = e^\lambda \quad (30)$$

while the initial conditions in (20, 21) is imposed differently on  $R(x, t)$  as

$$R(x, 0) = \begin{cases} \rho_b e^{-\lambda} & \text{for annealed ensemble,} \\ \frac{\rho_b}{G(x, 0)} & \text{for quenched ensemble.} \end{cases} \quad (31)$$

For both the ensembles, the spatial boundary condition in (25a, 25b) become,

$$G(x, t) - \frac{1}{\Gamma} \frac{\partial G(x, t)}{\partial x} = 1 \quad \text{and} \quad R(x, t) - \frac{1}{\Gamma} \frac{\partial R(x, t)}{\partial x} = \rho_a \quad \text{at } x = 0. \quad (32)$$

The solution of the  $G$ -variable in either of the ensembles is

$$G(x, t) = 1 + (e^\lambda - 1) \int_0^\infty dy g(x, y, 1 - t) \quad (33)$$

where

$$g(x, y, t) = 2 \int_0^\infty dz \frac{e^{-\pi^2 t z^2}}{\Gamma^2 + \pi^2 z^2} (\Gamma \sin \pi x z + \pi z \cos \pi x z) (\Gamma \sin \pi y z + \pi z \cos \pi y z) \quad (34)$$

is the Green's function of the diffusion equation on the semi-infinite line  $x > 0$  for the Robin boundary condition  $g - \Gamma^{-1} \partial_x g = 1$  at  $x = 0$ . (See details in Appendix B.)

In a similar way, the solution for the  $R$ -variable is obtained as

$$R(x, t) = \rho_a + (\rho_b e^{-\lambda} - \rho_a) \int_0^\infty dy g(x, y, t) \quad \text{for annealed ensemble,} \quad (35a)$$

$$R(x, t) = \rho_a + \int_0^\infty dy g(x, y, t) \left( \frac{\rho_b}{G(y, 0)} - \rho_a \right) \quad \text{for quenched ensemble.} \quad (35b)$$

For the annealed ensemble using the solution for the cgf in (17) we get

$$\begin{aligned} \frac{\mu_{\mathcal{A}}(\lambda)}{\sqrt{T}} &\simeq \Gamma \rho_a (e^\lambda - 1) \int_0^1 dt \int_0^\infty dy g(0, y, 1 - t) \\ &\quad + \rho_b (e^{-\lambda} - 1) \int_0^\infty dx \left( 1 - \int_0^\infty dy g(x, y, 1) \right). \end{aligned} \quad (36)$$

The last term in the equation above is re-expressed using an identity (see Appendix B for a proof)

$$\int_0^\infty dx \left( 1 - \int_0^\infty dy g(x, y, 1) \right) = \Gamma \int_0^1 dt \int_0^\infty dy g(0, y, 1 - t) \quad (37)$$

that leads to the expression for cgf in (3a). The ldf is plotted in figure 4 for different boundary rates  $\Gamma$ .

For the quenched ensemble the cgf in (17) takes the form

$$\begin{aligned} \frac{\mu_{\mathcal{Q}}(\lambda)}{\sqrt{T}} &\simeq \Gamma \rho_a (e^\lambda - 1) \int_0^1 dt \int_0^\infty dy g(0, y, 1 - t) \\ &\quad + \rho_b \int_0^\infty dx \log \left[ 1 + (e^{-\lambda} - 1) \left( 1 - \int_0^\infty dy g(x, y, 1) \right) \right]. \end{aligned} \quad (38)$$

The two integrals in the first term gives the  $\Omega_\Gamma$  in (3b), which leads to expression reported in (4a).

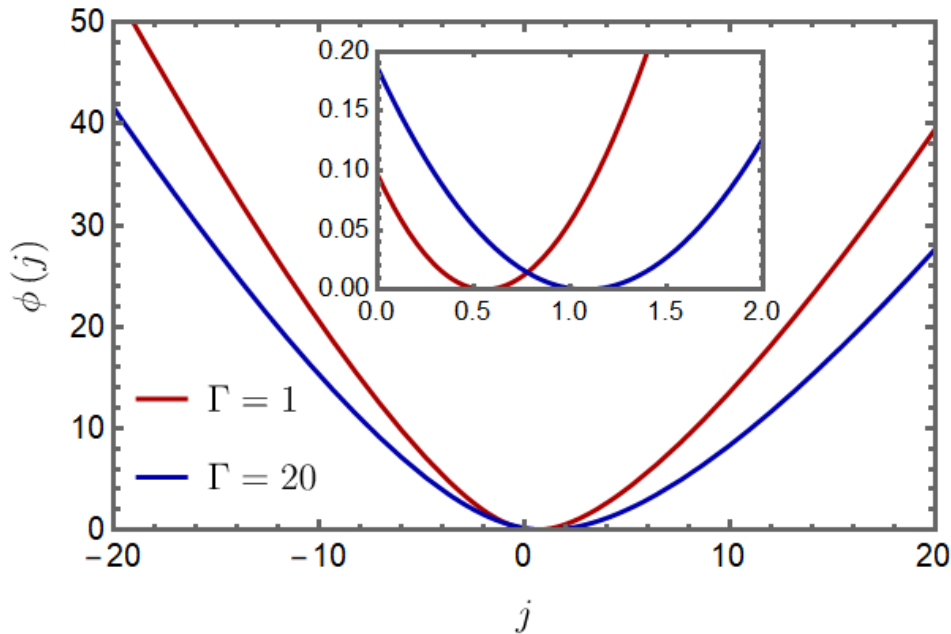


**Figure 4.** (color online) The large deviation function  $\phi(q)$  for the annealed ensemble with  $\rho_a = 2$  and  $\rho_b = 1$  for different values of  $\Gamma$  indicated in the *legend*. The inset shows a zoom-in plot near the minimum of the ldf to indicate the dependence of the average current on  $\Gamma$ .

### 3.1. Large deviations function

The ldf  $\phi(j)$  relates to the cgf by the Legendre-Fenchel transform (5). For the annealed case, using (3a) we get an explicit expression

$$\phi_{\mathcal{A}}(j) = j \log \frac{j + \sqrt{j^2 + 4\rho_a\rho_b\Omega_{\Gamma}^2}}{2\rho_a\Omega_{\Gamma}} - \frac{4\rho_a\rho_b\Omega_{\Gamma}^2}{j + \sqrt{j^2 + 4\rho_a\rho_b\Omega_{\Gamma}^2}} - j + (\rho_a + \rho_b)\Omega_{\Gamma} \quad (39)$$

where,  $\Omega_{\Gamma}$  is the boundary rate dependent factor defined in (3b). The ldf is plotted in figure 4 which illustrates the dependence on  $\Gamma$ .

For the quenched ensemble we obtain a parametric expression

$$\begin{aligned} \phi_{\mathcal{Q}}(j) = & \lambda\rho_a e^{\lambda}\Omega_{\Gamma} - \lambda\rho_b e^{-\lambda} \int_0^{\infty} dx \frac{W_{\Gamma}(x)}{1 + (e^{-\lambda} - 1)W_{\Gamma}(x)} \\ & - \rho_a (e^{\lambda} - 1)\Omega_{\Gamma} - \rho_b \int_0^{\infty} dx \log [1 + (e^{-\lambda} - 1)W_{\Gamma}(x)] \end{aligned} \quad (40)$$

with the current  $j$  depending on the  $\lambda$ -parameter via

$$j = \rho_a e^{\lambda}\Omega_{\Gamma} - \rho_b e^{-\lambda} \int_0^{\infty} dx \frac{W_{\Gamma}(x)}{1 + (e^{-\lambda} - 1)W_{\Gamma}(x)} \quad (41)$$

where  $W_{\Gamma}$  is defined in (4b).

**Remark:** The least-action path  $q(x, t) = G(x, t)R(x, t)$  with the solution (33, 35a, 35b) gives the most-probable density evolution contributing to an atypical value of  $Q_T =$

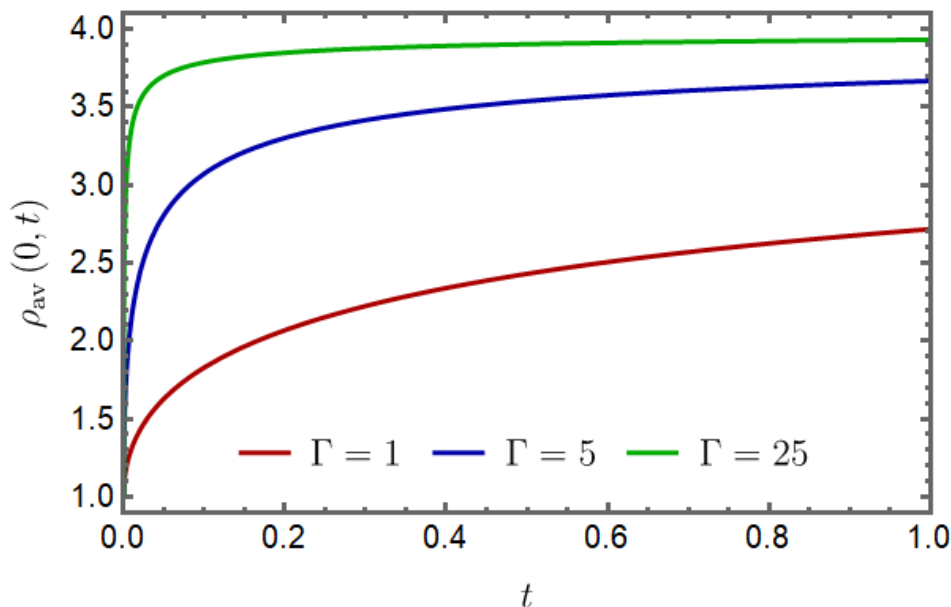


**Figure 5.** Time evolution of the average density (42) near the reservoir for different boundary rates  $\Gamma$  indicated in the *legend*. We have set  $\rho_a = 4$  and  $\rho_b = 1$ .

$\mu'(\lambda)$  for large  $T$  in the respective ensemble. For  $\lambda = 0$  the  $q(x, t)$  is the average density  $\rho_{\text{av.}}(x, t)$  which is identical in both ensembles and evolves as

$$\rho_{\text{av.}}(x, t) = \rho_a + \frac{2\Gamma(\rho_b - \rho_a)}{\pi} \int_0^\infty dz \frac{e^{-\pi^2 tz^2} (\Gamma \sin \pi xz + \pi z \cos \pi xz)}{z(\Gamma^2 + \pi^2 z^2)}. \quad (42)$$

At the boundary the density  $\rho_{\text{av.}}(0, t)$  is different from the reservoir density. A plot of its evolution is shown in figure 5.

#### 4. An exact microscopic calculation

The derivation we followed (Appendix A) for the variational formulation in (13, 14) rests on certain uncontrolled approximations to get the hydrodynamic limit. It is therefore important to verify the results in Sec. 3 using an independent exact analysis of the microscopic dynamics. Similar to the SSEP in figure 1, the nearest neighbour jump rates in the bulk sites for the non-interacting model are chosen as 1 where particles move without an exclusion interaction. The boundary site is coupled with the reservoir of density  $\rho_a$  which is modelled by the injection rate  $\gamma\rho_a$  from the reservoir and the extraction rate  $\gamma$  to the reservoir.

The site index of the lattice are denoted by positive integers  $i = 1, 2, 3, \dots$  and the microscopic time coordinates by  $0 \leq \tau \leq T$ . The occupancy of the  $i$ -th lattice site in the initial configuration is denoted by  $n_i$  which we draw from a Poisson distribution  $P(n_i) = \frac{\rho_b^{n_i} e^{-\rho_b}}{n_i!}$  with uniform average occupation  $\langle n_i \rangle = \rho_b$ .

Presence of the boundary makes the calculation slightly different from the analysis [13, 45] on an infinite line. If a particle is in the  $i$ -th lattice site, then either it exits

the lattice into the reservoir by time  $\tau$  or it continues to be somewhere in the lattice till time  $\tau$ . We denote the probability of such events by  $\mathcal{E}_i(\tau)$  (escape probability), and  $\mathcal{S}_i(\tau)$  (survival probability) respectively. Bearing in mind that the particles are non-interacting, we write the joint statistics in terms of single-particle statistics.

$$\begin{aligned} \langle e^{\lambda Q_T} \rangle_{\text{hist.}} &= \prod_{k=0}^{T/d\tau} [1 - \gamma \rho_a d\tau \mathcal{S}_1(T - kd\tau) + e^{\lambda} \gamma \rho_a d\tau \mathcal{S}_1(T - kd\tau)] \\ &\quad \times \prod_{i=1}^{\infty} [1 - \mathcal{E}_i(T) + e^{-\lambda} \mathcal{E}_i(T)]^{n_i} \end{aligned} \quad (43)$$

where we have discretized the total time duration  $T$  into infinitesimal intervals of length  $d\tau$ . The first product is the contribution from particles that are injected from the reservoir during the time interval  $[0, T]$  and the second product is the contribution from particles present in the initial state. In the vanishing  $d\tau$  limit,

$$\langle e^{\lambda Q_T} \rangle_{\text{hist.}} = \exp \left[ \gamma \rho_a (e^{\lambda} - 1) \int_0^T d\tau \mathcal{S}_1(\tau) \right] \prod_{i=1}^{\infty} [1 + (e^{-\lambda} - 1) \mathcal{E}_i(T)]^{n_i}. \quad (44)$$

The escape probabilities  $\mathcal{E}_i(\tau)$  are solution of the rate equation

$$\frac{d\mathcal{E}_i(\tau)}{d\tau} = \begin{cases} \mathcal{E}_2(\tau) - (1 + \gamma) \mathcal{E}_1(\tau) + \gamma & \text{for } i = 1, \\ \mathcal{E}_{i+1}(\tau) - 2\mathcal{E}_i(\tau) + \mathcal{E}_{i-1}(\tau) & \text{for } i \geq 2. \end{cases} \quad (45)$$

with the initial condition  $\mathcal{E}_i(0) = 0$ . The survival probability simply relates to the escape probability  $\mathcal{E}_i(\tau) + \mathcal{S}_i(\tau) = 1$ . Using this relation and (45) we find an useful identity

$$\gamma \int_0^T d\tau \mathcal{S}_1(\tau) = \sum_{i=1}^{\infty} \mathcal{E}_i(T) \quad (46)$$

that will be used shortly.

For an explicit expression of  $\mathcal{E}_i(T)$  we solve (45) using the Laplace transform

$$\widehat{\mathcal{E}}_i(s) \equiv \mathcal{L}[\mathcal{E}_i](s) := \int_0^{\infty} d\tau e^{-s\tau} \mathcal{E}_i(\tau) \quad (47)$$

which follows

$$s \widehat{\mathcal{E}}_i(s) = \begin{cases} \widehat{\mathcal{E}}_2(s) - (1 + \gamma) \widehat{\mathcal{E}}_1(s) + \frac{\gamma}{s} & \text{for } i = 1, \\ \widehat{\mathcal{E}}_{i+1}(s) - 2\widehat{\mathcal{E}}_i(s) + \widehat{\mathcal{E}}_{i-1}(s) & \text{for } i \geq 2. \end{cases} \quad (48)$$

The solution that vanishes at  $i \rightarrow \infty$  is

$$\widehat{\mathcal{E}}_i(s) = \frac{\gamma}{s} \left( \gamma + \frac{s}{2} + \sqrt{s + \frac{s^2}{4}} \right)^{-1} \left( 1 + \frac{s}{2} - \sqrt{s + \frac{s^2}{4}} \right)^{i-1}. \quad (49)$$

Inverting the Laplace transform to get  $\mathcal{E}_i(\tau)$  is hard. However, for the large  $T$  limit, asymptotic expressions for  $\mathcal{E}_i$  can be obtained.

#### 4.1. Annealed averaging

Averaging (44) over the initial configurations which are drawn from a Poisson distribution with an average  $\rho_b$ , we get

$$\begin{aligned} \langle \langle e^{\lambda Q_T} \rangle_{\text{hist.}} \rangle_{\text{init.}} &= \exp \left[ \gamma \rho_a (e^\lambda - 1) \int_0^T d\tau \mathcal{S}_1(\tau) \right] \\ &\times \sum_{n_i=0}^{\infty} \prod_{i=1}^{\infty} \left\{ [1 + (e^{-\lambda} - 1) \mathcal{E}_i(T)]^{n_i} \frac{\rho_b^{n_i} e^{-\rho_b}}{n_i!} \right\} \end{aligned} \quad (50)$$

which after simplifying and using (46) gives the cgf in (2) as

$$\mu_A(\lambda) = \gamma [\rho_a (e^\lambda - 1) + \rho_b (e^{-\lambda} - 1)] \int_0^T d\tau \mathcal{S}_1(\tau). \quad (51)$$

To compute the integral in the above expression we use  $\mathcal{S}_1(\tau) = 1 - \mathcal{E}_1(\tau)$  and write the Laplace transformation

$$\mathcal{L} \left[ \int_0^T d\tau \mathcal{S}_1(\tau) \right] (s) = \frac{1 - s \widehat{\mathcal{E}}_1(s)}{s^2} \simeq \frac{\sqrt{s}}{s^2 (\gamma + \sqrt{s})} \quad (52)$$

where we have used (49) with small  $s$ . In the large  $T$  limit the leading contribution from small  $s$ , which by taking the inverse Laplace transformation gives

$$\int_0^T d\tau \mathcal{S}_1(\tau) \simeq \frac{\sqrt{T}}{\gamma} \left( \frac{2}{\sqrt{\pi}} - \frac{1 - e^{\gamma^2 T} \text{erfc } \gamma \sqrt{T}}{\gamma \sqrt{T}} \right) \quad (53)$$

for large  $T$ . Using this asymptotic in (51) with  $\gamma = \frac{\Gamma}{\sqrt{T}}$  gives the expression (3a).

#### 4.2. Quenched averaging

Taking the logarithm of (44) and then averaging over the initial configurations

$$\begin{aligned} \langle \log [\langle e^{\lambda Q_T} \rangle_{\text{hist.}}] \rangle_{\text{init.}} &= \gamma \rho_a (e^\lambda - 1) \int_0^T d\tau \mathcal{S}_1(\tau) \\ &+ \sum_{n_i=0}^{\infty} \sum_{i=1}^{\infty} \left\{ \log [1 + (e^{-\lambda} - 1) \mathcal{E}_i(T)]^{n_i} \frac{\rho_b^{n_i} e^{-\rho_b}}{n_i!} \right\} \end{aligned} \quad (54)$$

we get the cgf (2) in the quenched case.

$$\mu_Q(\lambda) = \gamma \rho_a (e^\lambda - 1) \int_0^T d\tau \mathcal{S}_1(\tau) + \rho_b \sum_{i=1}^{\infty} \log [1 + (e^{-\lambda} - 1) \mathcal{E}_i(T)] \quad (55)$$

To obtain the leading asymptotic for large  $T$  in the parameter regime of our interest we set  $\gamma = \frac{\Gamma}{\sqrt{T}}$ . Asymptotic of the first term in (55) is given by (53) whereas for the second term we take the diffusive scaling  $\mathcal{E}_i(\tau) \simeq \mathcal{E}(\frac{i}{\sqrt{T}}, \frac{\tau}{T})$  and write

$$\frac{\mu_Q(\lambda)}{\sqrt{T}} = \rho_a (e^\lambda - 1) \Omega_\Gamma + \rho_b \int_0^\infty dx \log [1 + (e^{-\lambda} - 1) \mathcal{E}(x, 1)] \quad (56)$$

with  $\Omega_\Gamma$  defined in (3b).

## 5. Perturbation solution for the Symmetric Simple Exclusion Process

The variational problem (17) for SSEP is hard to solve explicitly. Corresponding variational problem on the infinite line [13] has been recently solved [12] using a remarkable connection to an integrable model. While the difference between the two variational problems is only in the spatial boundary condition, this small difference makes the semi-infinite geometry hard to solve at present.

In this article, we use a straightforward perturbation expansion in small  $\lambda$  to solve the variational problem order by order. This gives a systematic approach for the cumulants of the current. Similar perturbation expansion has been used for statistics of current [46] and activity [47] on an infinite line and tracer statistics in single file diffusion [48].

For  $\lambda = 0$ , the least-action solution for either ensembles is  $p(x, t) = 0$  and  $q(x, t) = \rho_{\text{av}}(x, t)$  given in (42) which follows (10a, 10b). For small  $\lambda$  we write a perturbation expansion

$$q = \rho_{\text{av}} + \lambda q_1 + \lambda^2 q_2 + \dots, \quad (57a)$$

$$p = \lambda p_1 + \lambda^2 p_2 + \dots. \quad (57b)$$

Substituting the expansion in (18a, 18b) gives the least-action path at the linear order

$$\frac{\partial p_1(x, t)}{\partial t} = -\frac{\partial^2 p_1(x, t)}{\partial x^2}, \quad (58a)$$

$$\frac{\partial q_1(x, t)}{\partial t} = \frac{\partial^2 q_1(x, t)}{\partial x^2} - \frac{\partial}{\partial x} \left( \sigma(\rho_{\text{av}}) \frac{\partial p_1(x, t)}{\partial x} \right), \quad (58b)$$

and at the quadratic order

$$\frac{\partial p_2(x, t)}{\partial t} = -\frac{\partial^2 p_2(x, t)}{\partial x^2} - \frac{\sigma'(\rho_{\text{av}})}{2} \left( \frac{\partial p_1(x, t)}{\partial x} \right)^2, \quad (59a)$$

$$\frac{\partial q_2(x, t)}{\partial t} = \frac{\partial^2 q_2(x, t)}{\partial x^2} - \frac{\partial}{\partial x} \left( q_1(x, t) \sigma'(\rho_{\text{av}}) \frac{\partial p_1(x, t)}{\partial x} + \sigma(\rho_{\text{av}}) \frac{\partial p_2(x, t)}{\partial x} \right). \quad (59b)$$

The Robin boundary conditions (19a, 19b) gives the spatial boundary condition for these perturbation fields at  $x = 0$ . At the linear order, we obtain

$$p_1(0, t) - \frac{1}{\Gamma} \frac{\partial p_1(x, t)}{\partial x} \Big|_{x=0} = 0, \quad (60a)$$

$$q_1(0, t) - \frac{1}{\Gamma} \frac{\partial q_1(x, t)}{\partial x} \Big|_{x=0} = p_1(0, t) (\rho_a - \rho_{\text{av}}(0, t)) (1 - 2\rho_{\text{av}}(0, t)) := C_1(t). \quad (60b)$$

while at the quadratic order, we obtain

$$p_2(0, t) - \frac{1}{\Gamma} \frac{\partial p_2(x, t)}{\partial x} \Big|_{x=0} = \frac{p_1^2(0, t) (1 - 2\rho_a)}{2} := C_2(t) \quad (61a)$$

$$\begin{aligned} q_2(0, t) - \frac{1}{\Gamma} \frac{\partial q_2(x, t)}{\partial x} \Big|_{x=0} &= \frac{p_1^2(0, t) (\rho_a - \rho_{\text{av}}(0, t))}{2} - p_1(0, t) q_1(0, t) (1 + 2\rho_a - 4\rho_{\text{av}}(0, t)) \\ &\quad + p_1^2(0, t) (1 - 2\rho_a) \rho_{\text{av}}(0, t) (1 - \rho_{\text{av}}(0, t)) \\ &\quad + p_2(0, t) (\rho_a - \rho_{\text{av}}(0, t)) (1 - 2\rho_{\text{av}}(0, t)) := C_3(t) \end{aligned} \quad (61b)$$

In the perturbation expansion, the fields at certain order in  $\lambda$  only depends on the lower-order fields and therefore they can be systematically solved order-by-order. Using the perturbation expansion (57b) in the expression (22) gives a series solution the cgf

$$\mu(\lambda) = \lambda \langle Q_T \rangle + \frac{\lambda^2}{2!} \langle Q_T^2 \rangle + \frac{\lambda^3}{3!} \langle Q_T^3 \rangle + \dots \quad (62)$$

where the coefficients in each order are by definition the cumulants of the current. A similar hierarchical dependence prevails. Namely, the first cumulant  $\langle Q_T \rangle$  are expressed in terms of leading order fields  $\rho_{\text{av}}$ , the second cumulant  $\langle Q_T^2 \rangle$  in terms of  $(q_1, p_1)$ , and so on.

For the quenched ensemble, the expression for the average is

$$\frac{\langle Q_T \rangle_{\mathcal{Q}}}{\sqrt{T}} \simeq - \int_0^1 dt \left. \frac{\partial \rho_{\text{av}}(x, t)}{\partial x} \right|_{x=0}, \quad (63)$$

where the average density is written as  $\rho_{\text{av}}(x, t) = \rho_a + (\rho_b - \rho_a) \int_0^\infty dy g(x, y, t)$  with the Green's function as in (34). The expression in (63) can be explicitly evaluated and we arrive at the result reported in (6). Note that this is the same expression we obtained for the non-interacting particles.

Similarly from higher powers of  $\lambda$ , we obtain the variance

$$\begin{aligned} \frac{\langle Q_T^2 \rangle_{\mathcal{Q}}}{\sqrt{T}} &\simeq 2 \int_0^1 dt \int_0^\infty dx \rho_{\text{av}}(x, t) (1 - \rho_{\text{av}}(x, t)) \left( \frac{\partial p_1(x, t)}{\partial x} \right)^2 \\ &\quad + \Gamma \int_0^1 dt B_2[\rho_{\text{av}}(0, t), p_1(0, t)] \end{aligned} \quad (64)$$

with

$$B_2[\rho_{\text{av}}, p_1] = p_1^2 (2\rho_{\text{av}}\rho_a - \rho_{\text{av}} - \rho_a), \quad (65)$$

the third cumulant

$$\begin{aligned} \frac{\langle Q_T^3 \rangle_{\mathcal{Q}}}{\sqrt{T}} &\simeq 6 \int_0^1 dt \int_0^\infty dx \left[ q_1(x, t) (1 - 2\rho_{\text{av}}(x, t)) \left( \frac{\partial p_1(x, t)}{\partial x} \right)^2 \right] \\ &\quad + \Gamma \int_0^1 dt B_3[\rho_{\text{av}}(0, t), p_1(0, t), q_1(0, t), p_2(0, t)] \end{aligned} \quad (66)$$

with

$$\begin{aligned} B_3[\rho_{\text{av}}, p_1, q_1, p_2] &= p_1 \left( 2\rho_{\text{av}}p_1^2 + 12\rho_{\text{av}}p_2\rho_a - 6\rho_{\text{av}}p_2 - 2p_1^2\rho_a \right. \\ &\quad \left. + 6q_1p_1\rho_a - 3q_1p_1 - 6p_2\rho_a \right), \end{aligned} \quad (67)$$

and so on.

For the annealed ensemble, a similar expansion in the  $\lambda$ -parameter gives the cumulants. The average current is same as given in (63) and with the same explicit expression as in (6). The expressions for the higher cumulants are however different and are provided in the section 5.2.



## 5.1. Quenched ensemble

The difference in the variational problem comes from the temporal boundary condition (20, 21). For the quenched case, the temporal boundary condition (21) gives the condition for the perturbation fields

$$p_1(x, 1) = 1, \quad p_2(x, 1) = 0, \dots, \quad (68a)$$

$$q_1(x, 0) = 0, \quad q_2(x, 0) = 0 \dots \quad (68b)$$

The optimal fields can be solved order by order for arbitrary  $\Gamma$ , first solving for  $p_k$  at a perturbation order  $k$  in terms of the green's function  $g(x, y, t)$  in (34) and then  $q_k$  in terms of  $\tilde{g}(x, y, t)$  in (B.8). However, their expressions are cumbersome and not informative for the moment. We present rest of the analysis for the fast coupling limit ( $\Gamma \rightarrow \infty$ ) where we find explicit expressions for the first few cumulants. In this limit, the boundary conditions in (60a - 61b) reduce to Dirichlet boundary conditions on the perturbation fields. Some of the formal expressions for the slow coupling limit are presented in the Appendix.

The mean (63) in the fast coupling limit yields

$$\frac{\langle Q_T \rangle}{\sqrt{T}} \simeq (\rho_a - \rho_b) \frac{2}{\sqrt{\pi}} \quad (69)$$

which is the  $\Gamma \rightarrow \infty$  limit of (6). The variance (64) in the fast coupling limit is

$$\frac{\langle Q_T^2 \rangle_{\mathcal{Q}}}{\sqrt{T}} \simeq \frac{1}{\pi} \int_0^1 dt \int_0^\infty dx \sigma(\rho_{\text{av}}(x, t)) \frac{e^{-x^2/2(1-t)}}{1-t} \quad (70)$$

with  $\sigma(\rho) = 2\rho(1 - \rho)$  and

$$\rho_{\text{av}}(x, t) = \rho_a + (\rho_b - \rho_a) \operatorname{erf} \left( \frac{x}{2\sqrt{t}} \right) \quad (71)$$

Completing the integration gives the explicit expression as reported in (8).

The third cumulant (66) in the fast coupling limit

$$\frac{\langle Q_T^3 \rangle_{\mathcal{Q}}}{\sqrt{T}} \simeq 3 \int_0^1 dt \int_0^\infty dx \sigma'(\rho_{\text{av}}(x, t)) \frac{e^{-x^2/2(1-t)}}{\pi(1-t)} q_1(x, t) \quad (72)$$

where  $q_1(x, t) = -\partial_x \psi_1(x, t)$  with

$$\psi_1(x, t) = \int_0^t ds \int_0^\infty dy \sigma(\rho_{\text{av}}(y, s)) \frac{e^{-y^2/4(1-s)} e^{-(y-x)^2/4(t-s)} + e^{-(y+x)^2/4(t-s)}}{\sqrt{\pi(1-s)} \sqrt{4\pi(t-s)}} \quad (73)$$

For  $\rho_b = 0$ , the formal result (72) is consistent with the explicit expression (9) which is derived by extracting integral identities from a comparison with the hydrodynamic formulation on the infinite line [13] and using the known results [11].

**Remark:** The expressions in (70-73) are written such that they hold for all systems with unit diffusivity  $D(\rho) = 1$  and a generic mobility  $\sigma(\rho)$ .

## 5.2. Annealed ensemble

In the annealed ensemble, the boundary condition (19b) gives the same conditions (68a) for the  $p$ -field at various perturbation orders, whereas for perturbative  $q$ -fields it gives

$$q_1(x, 0) = \frac{\sigma(\rho_b)(p_1(x, 0) - 1)}{2}, \quad (74)$$

$$q_2(x, 0) = \frac{\sigma(\rho_b)p_2(x, 0)}{2} + \frac{\sigma'(\rho_b)\sigma(\rho_b)(p_1(x, 0) - 1)^2}{8}, \dots \quad (75)$$

The solutions for these perturbation fields are straightforward to write in terms of the green's functions  $g(x, y, t)$  in (34) and  $\tilde{g}(x, y, t)$  in (B.8). We present here only the results for fast coupling limit, which have simpler expression.

In the fast coupling limit, the variance in the annealed case differs from that in the quenched case.

$$\frac{\langle Q_T^2 \rangle_{\mathcal{A}}}{\sqrt{T}} \simeq \frac{2 - \sqrt{2}}{\sqrt{\pi}} \sigma(\rho_b) + \frac{\langle Q_T^2 \rangle_{\mathcal{Q}}}{\sqrt{T}} \quad (76)$$

with  $\langle Q_T^2 \rangle_{\mathcal{Q}}$  given in (70).

The third cumulant in the fast coupling limit is given by

$$\frac{\langle Q_T^3 \rangle_{\mathcal{A}}}{\sqrt{T}} \simeq E + \frac{\langle Q_T^3 \rangle_{\mathcal{Q}}}{\sqrt{T}} \quad (77a)$$

with the difference

$$E = \int_0^\infty dx \left( 6\tilde{g}_\infty(x, 0, 1)\psi_2(x, 0) - \frac{12q_1(x, 0)q_2(x, 0)}{\sigma(\rho_b)} + \frac{2\sigma'(\rho_b)q_1^3(x, 0)}{\sigma^2(\rho_b)} \right) - 3 \int_0^1 dt \int_0^\infty dx \sigma'(\rho_{\text{av}}(x, t)) \frac{e^{-x^2/2(1-t)}}{\pi(1-t)} \int_0^\infty dy \partial_x \tilde{g}_\infty(x, y, t) \psi_1(y, 0) \quad (77b)$$

where  $q_1(x, t) = -\partial_x \psi_1(x, t)$  with

$$\psi_1(x, t) = \int_0^t ds \int_0^\infty dy \tilde{g}_\infty(x, y, t-s) \sigma(\rho_{\text{av}}(y, s)) \frac{e^{-y^2/4(1-s)}}{\sqrt{\pi(1-s)}} + \int_0^\infty dy \tilde{g}_\infty(x, y, t) \psi_1(y, 0), \quad (77c)$$

and  $q_2(x, t) = -\partial_x \psi_2(x, t)$  with

$$\psi_2(x, t) = \int_0^t ds \int_0^\infty dy \tilde{g}_\infty(x, y, t-s) \sigma'(\rho_{\text{av}}(y, s)) q_1(y, s) \frac{e^{-y^2/4(1-s)}}{\sqrt{\pi(1-s)}} + \int_0^t ds \int_0^\infty dy \tilde{g}_\infty(x, y, t-s) \sigma(\rho_{\text{av}}(y, s)) \frac{\partial p_2(y, s)}{\partial y} + \int_0^\infty dy \tilde{g}_\infty(x, y, t) \psi_2(y, 0) \quad (77d)$$

and

$$p_2(x, t) = \int_t^1 ds \int_0^\infty dy g_\infty(x, y, s-t) \frac{\sigma'(\rho_{\text{av}}(y, 1-s)) e^{-y^2/2s}}{2} \frac{1}{\pi s} \quad (77e)$$

with

$$g_\infty(x, y, t) = \frac{e^{-(y-x)^2/4t} - e^{-(y+x)^2/4t}}{\sqrt{4\pi t}} \quad \text{and} \quad \tilde{g}_\infty(x, y, t) = \frac{e^{-(y-x)^2/4t} + e^{-(y+x)^2/4t}}{\sqrt{4\pi t}} \quad (77f)$$

The formal expression (77a) for the third cumulant is consistent with the explicit expression (9). We have carried out the integration for  $(\rho_a, \rho_b) \equiv (\frac{1}{2}, 0)$  by comparing similar results for the hydrodynamic formulation on the infinite line [13] and using the known results [11]. The expression for arbitrary densities is then obtained using the symmetry of the annealed cgf discussed in the last remark in section 2.

## 6. Conclusion

In this article we examined a one dimensional semi-infinite SSEP connected to a particle reservoir at one end with a varied coupling strength. We carefully showed (section 2) how to apply the well-known MFT approach in this non-equilibrium context, particularly for studying current fluctuations in the large time limit. In the MFT formalism, the slow coupling with reservoir introduces an additional contribution to the hydrodynamic Action. For the SSEP and the non-interacting case we have shown (Appendix A) how this term can be obtained using an analysis which is simple to generalize for similar transport models. For the non-interacting case the variational problem of the MFT is solved giving explicit expression for the cgf of current (section 3). Not-surprisingly the analysis is able to capture the long-term memory of the initial condition reported earlier in similar context. For an indirect verification of the hydrodynamic theory we have reproduced the results for the non-interacting case using an exact solution starting with the microscopic dynamics (section 4). For the SSEP both the variational and microscopic solutions are hard to obtain at this moment. We have used a standard perturbation method to derive the results of the first few cumulants of the current (section 5).

The perturbation approach is a systematic way to obtain the cumulants order by order. Similar to that on the finite [7] and the infinite line [13], the cgf of current for the annealed ensemble of the SSEP depends on the parameters  $\rho_a$ ,  $\rho_b$ , and  $\lambda$  through a single parameter  $\omega = \rho_a(1 - \rho_b)(e^\lambda - 1) + \rho_b(1 - \rho_a)(e^{-\lambda} - 1)$ . This would mean that the cgf has a series expansion in powers of  $\omega$  which may be simpler to predict. The perturbation solution of the variational problem is one way to obtain the leading terms of that series.

The appealing idea of the hydrodynamic approach of the MFT is its generality. For the semi-infinite line with the slow coupling our presentation is easily extendable for other diffusive transport models. For example, the exclusion process with weak drift, the KMP model of heat-transport, the Zero-Range process model of condensation, and the inclusion process have a similar hydrodynamic description and it would be of interest to obtain their results for current fluctuations.

The aspect of integrability of the variational problem within MFT has seen a remarkable progress in the recent years [12, 17, 49]. On the infinite lattice, the variational

problem for the SSEP has been solved [12]. Corresponding solution for the semi-infinite geometry still poses a challenging open problem.

## Acknowledgments

We acknowledge support of the Department of Atomic Energy, Government of India, under Project Identification No. RTI-4002. TS acknowledges many insightful discussions with Bernard Derrida about the results in this work. Many crucial ideas, especially the importance of considering the slow coupling, the derivation of the hydrodynamic action, and the microscopic solution for the non-interacting case have originated from such discussions.

## Appendix A. A derivation of the hydrodynamic-Action for the SSEP

We present a non-rigorous, but simple approach for deriving the fluctuating hydrodynamics description for SSEP. A similar analysis for stochastic processes was discussed in an earlier work of Lefèvre and Biroli [50]. We follow our notation in this article for the SSEP on a discrete lattice with the sites denoted by  $i = 1, 2, 3, \dots, \infty$  and the microscopic time denoted by  $\tau$ . Jump rates are denoted in figure 1. The configuration of the system is given by the set  $\{n_i(\tau)\}$  with  $i$  running through all the lattice indices where  $n_i(\tau)$  denotes the occupancy of the  $i$ -th lattice site at the given instant of time  $\tau$ . Here,  $n_i$  is equal to 0 if the site is empty whereas it equals to 1 when the site is filled with one particle. For the SSEP, there can be at most one particle in a site at a given time. The total measurement time  $T$  is broken into  $M$  number of infinitesimal steps each of a duration  $d\tau$ . This allows us to denote any instant of the microscopic time  $\tau$  as  $k d\tau$  such that  $k = 0, 1, 2, \dots, M$  with  $M d\tau = T$  being the final time step.

The conservation law for the number of particles states that

$$n_i(\tau + d\tau) - n_i(\tau) = Y_{i-1}(\tau) - Y_i(\tau) \quad (\text{A.1})$$

where  $Y_i(\tau)$  denotes the flux of particles in the infinitesimal time window between  $\tau$  and  $\tau + d\tau$  across the bond connecting the  $i$ -th and the  $(i + 1)$ -th sites. The  $Y_0(\tau)$  denotes the influx of particles from the reservoir to the boundary site  $i = 1$ .

In our notation, the net current of particles from the reservoir in time  $T$  is  $Q_T = \sum_{k=0}^M Y_0(k d\tau)$  and using (A.1) we get

$$Q_T = \sum_{i=1}^{\infty} (n_i(T) - n_i(0)). \quad (\text{A.2})$$

This is the microscopic analogue of (12).

In an infinitesimal time step  $d\tau$ , the  $Y_i(\tau)$  can have three possible values: 0 or  $\pm 1$ .

In the bulk of the lattice (i.e., for  $i \geq 1$ ),

$$Y_i(\tau) = \begin{cases} 1 & \text{with prob. } n_i(\tau) (1 - n_{i+1}(\tau)) d\tau \\ -1 & \text{with prob. } n_{i+1}(\tau) (1 - n_i(\tau)) d\tau \\ 0 & \text{with prob. } 1 - [n_i(\tau) (1 - n_{i+1}(\tau)) + n_{i+1}(\tau) (1 - n_i(\tau))] d\tau \end{cases} \quad (\text{A.3})$$

Across the system-reservoir boundary

$$Y_0(\tau) = \begin{cases} 1 & \text{with prob. } \gamma \rho_a (1 - n_1(\tau)) d\tau \\ -1 & \text{with prob. } \gamma n_1(\tau) (1 - \rho_a) d\tau \\ 0 & \text{with prob. } 1 - \gamma [\rho_a (1 - n_1(\tau)) + n_1(\tau) (1 - \rho_a)] d\tau \end{cases} \quad (\text{A.4})$$

The generating function  $\langle e^{\lambda Q_T} \rangle_{\text{hist.}}$  where the average is over all history starting with a fixed initial configuration  $\{n_i(0)\}$  is

$$\langle e^{\lambda Q_T} \rangle_{\text{hist}} = \int \mathcal{D}[n, Y] \left\langle \prod_{i=1}^{\infty} e^{\lambda [n_i(T) - n_i(0)]} \times \prod_{k=0}^{M-1} \delta_{n_i(k d\tau + d\tau) - n_i(k d\tau), Y_{i-1}(k d\tau) - Y_i(k d\tau)} \right\rangle_{[Y]} \quad (\text{A.5})$$

where the path integral measures are defined as

$$\int \mathcal{D}[n] = \prod_{k=1}^M \prod_{i=1}^{\infty} \sum_{n_i(k d\tau)=0}^1 \quad \text{and} \quad \int \mathcal{D}[Y] = \prod_{k=0}^{M-1} \prod_{i=0}^{\infty} \sum_{Y_i(k d\tau)=-1}^1 \quad (\text{A.6})$$

The  $\langle \rangle_{[Y]}$  denotes average over all evolution of  $\{Y_i(\tau)\}$  with appropriate probability weight.

Using an integral representation of Kronecker delta  $\delta_{a,b} = \frac{1}{2\pi i} \int_{-i\pi}^{i\pi} dz e^{-z(a-b)}$ , for integers  $a$  and  $b$ , we rewrite the expression

$$\langle e^{\lambda Q_T} \rangle_{\text{hist}} = \int \mathcal{D}[n, \hat{n}] e^{\lambda \sum_{i=1}^{\infty} (n_i(T) - n_i(0))} e^{-\sum_{k=0}^{M-1} \sum_{i=1}^{\infty} \hat{n}_i(k d\tau) (n_i(k d\tau + d\tau) - n_i(k d\tau))} \times \int \mathcal{D}[Y] \left\langle e^{\sum_{k=0}^{M-1} \sum_{i=1}^{\infty} \hat{n}_i(k d\tau) (Y_{i-1}(k d\tau) - Y_i(k d\tau))} \right\rangle_{[Y]} \quad (\text{A.7})$$

with the path integral measure on  $\hat{n}$  defined as

$$\int \mathcal{D}[\hat{n}] = \prod_{k=0}^{M-1} \prod_{i=1}^{\infty} \frac{1}{2\pi i} \int_{-i\pi}^{i\pi} d\hat{n}_i(k d\tau) \quad (\text{A.8})$$

To compute the average over  $Y$  we rearrange the terms in the exponential

$$\begin{aligned} & \sum_{i=1}^{\infty} \hat{n}_i(k d\tau) (Y_{i-1}(k d\tau) - Y_i(k d\tau)) \\ &= \hat{n}_1(k d\tau) Y_0(k d\tau) + \sum_{i=1}^{\infty} (\hat{n}_{i+1}(k d\tau) - \hat{n}_i(k d\tau)) Y_i(k d\tau) \end{aligned} \quad (\text{A.9})$$

and write

$$\begin{aligned} & \left\langle e^{\sum_{k=0}^{M-1} \sum_{i=1}^{\infty} [\hat{n}_i(k \, d\tau) (Y_{i-1}(k \, d\tau) - Y_i(k \, d\tau))]} \right\rangle_{[Y]} \\ &= \prod_{k=0}^{M-1} \left\langle \exp(\hat{n}_1(k \, d\tau) Y_0(k \, d\tau)) \right\rangle_{Y_0} \prod_{i=1}^{\infty} \left\langle \exp[(\hat{n}_{i+1}(k \, d\tau) - \hat{n}_i(k \, d\tau)) Y_i(k \, d\tau)] \right\rangle_{[Y_i]} \end{aligned} \quad (\text{A.10})$$

For the bulk sites ( $i > 0$ ) using the probability weight in (A.3) we get

$$\begin{aligned} & \left\langle \exp[(\hat{n}_{i+1}(k \, d\tau) - \hat{n}_i(k \, d\tau)) Y_i(k \, d\tau)] \right\rangle_{[Y_i]} \\ &= \exp \left\{ d\tau \left[ (e^{\hat{n}_{i+1}(k \, d\tau) - \hat{n}_i(k \, d\tau)} - 1) n_i(k \, d\tau) (1 - n_{i+1}(k \, d\tau)) \right. \right. \\ & \quad \left. \left. + (e^{\hat{n}_i(k \, d\tau) - \hat{n}_{i+1}(k \, d\tau)} - 1) n_{i+1}(k \, d\tau) (1 - n_i(k \, d\tau)) \right] \right\} \end{aligned} \quad (\text{A.11})$$

and for the boundary using (A.4) we get

$$\begin{aligned} \left\langle \exp(\hat{n}_1(k \, d\tau) Y_0(k \, d\tau)) \right\rangle_{Y_0} &= \exp \left\{ \gamma \, d\tau \left[ (e^{\hat{n}_1(k \, d\tau)} - 1) \rho_a (1 - n_1(k \, d\tau)) \right. \right. \\ & \quad \left. \left. + (e^{-\hat{n}_1(k \, d\tau)} - 1) n_1(k \, d\tau) (1 - \rho_a) \right] \right\} \end{aligned} \quad (\text{A.12})$$

Using (A.11, A.12) in (A.7) and taking the continuous time limit  $d\tau \rightarrow 0$ , we get

$$\begin{aligned} \langle e^{\lambda Q_T} \rangle_{\text{hist}} &= \int \mathcal{D}[n, \hat{n}] \exp \left[ \lambda \sum_{i=1}^{\infty} (n_i(T) - n_i(0)) \right] \\ & \quad \exp \left\{ - \int_0^T d\tau \left[ \left( \sum_{i=1}^{\infty} \hat{n}_i(\tau) \frac{dn_i(\tau)}{d\tau} \right) - \mathcal{H}[n(\tau), \hat{n}(\tau)] \right] \right\} \end{aligned} \quad (\text{A.13})$$

where the effective Hamiltonian  $\mathcal{H} = \mathcal{H}_{\text{bulk}} + \mathcal{H}_{\text{bdry}}$  with the bulk contribution given by

$$\begin{aligned} \mathcal{H}_{\text{bulk}} &= \sum_{i=1}^{\infty} \left[ n_i(\tau) (1 - n_{i+1}(\tau)) (e^{\hat{n}_{i+1}(\tau) - \hat{n}_i(\tau)} - 1) \right. \\ & \quad \left. + n_{i+1}(\tau) (1 - n_i(\tau)) (e^{\hat{n}_i(\tau) - \hat{n}_{i+1}(\tau)} - 1) \right] \end{aligned} \quad (\text{A.14})$$

and the effective boundary Hamiltonian is

$$\mathcal{H}_{\text{bdry}} = \gamma \left[ \rho_a (1 - n_1(\tau)) (e^{\hat{n}_1(\tau)} - 1) + n_1(\tau) (1 - \rho_a) (e^{-\hat{n}_1(\tau)} - 1) \right]. \quad (\text{A.15})$$

In the macroscopic scale  $(x, t) \equiv \left( \frac{i}{\sqrt{T}}, \frac{\tau}{T} \right)$ , assuming convergence to slowly varying hydrodynamic fields  $n_i(\tau) \rightarrow \rho(x, t)$  and  $\hat{n}_i(\tau) \rightarrow \hat{\rho}(x, t)$ , and following gradient expansion we arrive at the leading asymptotic of the generating function for large  $T$ , given in (14) with the case  $\mathcal{F} = 0$ .

**Remark:** In taking the continuous time limit we have written

$$\sum_{k=0}^{M-1} \hat{n}_i(k \, d\tau) [n_i(k \, d\tau + d\tau) - n_i(k \, d\tau)] \rightarrow \int_0^T d\tau \hat{n}_i(\tau) \frac{dn_i(\tau)}{d\tau}. \quad (\text{A.16})$$

Considering that  $n_i$  is either 0 or 1, the  $\frac{dn_i(\tau)}{d\tau}$  is ill defined. An interpretation of (A.13) may be drawn by defining the probability measure with respect to another

simpler process. For example, a particle deposition-evaporation process on the infinite lattice with unit rate and simple exclusion has similar path probability with an effective Hamiltonian

$$\mathcal{H}_{\text{DE}}[n_i(\tau), \hat{n}_i(\tau)] = (1 - n_i(\tau)) (e^{\hat{n}_i(\tau)} - 1) + n_i(\tau) (e^{-\hat{n}_i(\tau)} - 1). \quad (\text{A.17})$$

Then the Radon-Nikodym derivative of the path-probability for SSEP with respect to the deposition-evaporation process is well-defined.

### Appendix A.1. Non-Interacting particles

We proceed in the same manner as we did for the SSEP in the previous section. The main difference comes in the probabilities with which the particle flux takes the possible values.

The particle flux for the bulk lattice sites i.e.,  $i \geq 1$  at any time  $\tau$  can have three possible values with certain probabilities given by

$$Y_i(\tau) = \begin{cases} 1 & \text{with probability } n_i(\tau) d\tau \\ -1 & \text{with probability } n_{i+1}(\tau) d\tau \\ 0 & \text{with probability } 1 - (n_i(\tau) + n_{i+1}(\tau)) d\tau \end{cases} \quad (\text{A.18})$$

On the other hand, across the system-reservoir boundary i.e., for  $i = 0$  we have

$$Y_0(\tau) = \begin{cases} 1 & \text{with probability } \alpha d\tau = \gamma \rho_a d\tau \\ -1 & \text{with probability } \gamma n_1(\tau) d\tau \\ 0 & \text{with probability } 1 - \gamma (\rho_a + n_1(\tau)) d\tau \end{cases} \quad (\text{A.19})$$

Following a similar analysis as presented for the SSEP we arrive at the cgf (A.13) with

$$\mathcal{H}_{\text{bulk}}[n, \hat{n}] = (e^{\hat{n}_{i+1}(\tau) - \hat{n}_i(\tau)} - 1) n_i(\tau) + (e^{\hat{n}_i(\tau) - \hat{n}_{i+1}(\tau)} - 1) n_{i+1}(\tau) \quad (\text{A.20})$$

$$\mathcal{H}_{\text{bdry}}[n, \hat{n}] = \gamma [(e^{\hat{n}_1(\tau)} - 1) \rho_a + (e^{-\hat{n}_1(\tau)} - 1) n_1] \quad (\text{A.21})$$

In the hydrodynamic limit, this leads to the cgf in (12-15) with  $D(q) = 1$  and  $\sigma(q) = 2q$  and the boundary hamiltonian (24).

## Appendix B. The Green's function

The Green's function  $g(x, y, t)$  in (34) is the solution of the diffusion equation

$$\frac{\partial g(x, y, t)}{\partial t} = \frac{\partial^2 g(x, y, t)}{\partial x^2} \quad (\text{B.1})$$

on the semi-infinite line  $x > 0$  with the spatial boundary conditions

$$g(x, y, t) - \frac{1}{\Gamma} \frac{\partial g(x, y, t)}{\partial x} = 0 \quad \text{at } x = 0 \quad \text{and} \quad (\text{B.2})$$

$$g(x, y, t) = 0 \quad \text{at } x = \infty. \quad (\text{B.3})$$

and the initial condition

$$g(x, y, 0) = \delta(x - y) \quad (\text{B.4})$$

The solution (34) is obtained by spectral decomposition of the diffusion operator.

We have not been able to complete the integration in (34) over the  $z$ -variable for arbitrary  $\Gamma$ . In the two limiting cases, the green's function has an explicit expression: for the fast coupling limit ( $\Gamma \rightarrow \infty$ )

$$g(x, y, t) = \frac{e^{-(y-x)^2/4t} - e^{-(y+x)^2/4t}}{\sqrt{4\pi t}} \quad (\text{B.5})$$

which satisfies diffusion equation with absorbing boundary at  $x = 0$ , and for the slow coupling limit ( $\Gamma \rightarrow 0$ )

$$g(x, y, t) = \frac{e^{-(y-x)^2/4t} + e^{-(y+x)^2/4t}}{\sqrt{4\pi t}} \quad (\text{B.6})$$

which satisfies diffusion equation with reflecting boundary at  $x = 0$ .

The solution of the perturbation fields  $q_1$  and  $q_2$  in (57b) are expressed in terms of a second green's function  $\tilde{g}(x, y, t)$ , which is the solution of the diffusion equation as for the  $g(x, y, t)$  with the only difference in the boundary condition

$$\frac{\partial \tilde{g}(x, y, t)}{\partial x} - \frac{1}{\Gamma} \frac{\partial^2 \tilde{g}(x, y, t)}{\partial x^2} = 0 \quad \text{at } x = 0. \quad (\text{B.7})$$

The corresponding solution is

$$\tilde{g}(x, y, t) = 2 \int_0^\infty dz \left[ \frac{e^{-\pi^2 tz^2}}{\Gamma^2 + \pi^2 z^2} (\Gamma \cos \pi xz - \pi z \sin \pi xz) (\Gamma \cos \pi yz - \pi z \sin \pi yz) \right] \quad (\text{B.8})$$

### Appendix C. Derivation of the identity (37)

Using (B.1), we write

$$\frac{\partial}{\partial t} \left( 1 - \int_0^\infty dy g(x, y, 1-t) \right) = \frac{\partial^2}{\partial x^2} \int_0^\infty dy g(x, y, 1-t) \quad (\text{C.1})$$

Integrating both sides over  $t \in [0, 1]$ , we get

$$- \left( 1 - \int_0^\infty dy g(x, y, 1) \right) = \frac{\partial^2}{\partial x^2} \int_0^1 dt \int_0^\infty dy g(x, y, 1-t) \quad (\text{C.2})$$

where we have used (B.4) so that the LHS vanishes at  $t = 1$ . Integrating over  $x \in [0, \infty)$ , we obtain

$$\begin{aligned} - \int_0^\infty dx \left( 1 - \int_0^\infty dy g(x, y, 1) \right) &= \left( \frac{\partial}{\partial x} \int_0^1 dt \int_0^\infty dy g(x, y, t) \right) \Big|_{x=\infty} \\ &\quad - \left( \frac{\partial}{\partial x} \int_0^1 dt \int_0^\infty dy g(x, y, t) \right) \Big|_{x=0} \end{aligned} \quad (\text{C.3})$$

Using (B.3) such that at  $x = \infty$ , the slope of the Green's function vanishes and (B.2) for  $x = 0$ , the above reduces to (37).



## Appendix D. The average density profile

Recently, there have been much interest [26–33] to find the effect of slow coupling to a reservoir on the hydrodynamic description for the average density of the SSEP. Here we give a straightforward proof of (10a, 10b) for the SSEP in a semi-infinite lattice  $i \in \mathbb{Z}^+$  illustrated in figure 1.

The average occupancy  $\langle n_i(\tau) \rangle$  of the  $i$ -th lattice site at time  $\tau$  evolves according to the rate equation

$$\frac{d \langle n_i(\tau) \rangle}{d\tau} = \begin{cases} -(1 + \gamma) \langle n_1(\tau) \rangle + \langle n_2(\tau) \rangle + \gamma \rho_a & \text{for } i = 1 \\ \langle n_{i-1}(\tau) \rangle - 2 \langle n_i(\tau) \rangle + \langle n_{i+1}(\tau) \rangle & \text{for } i \geq 2 \end{cases} \quad (\text{D.1})$$

At  $\tau \rightarrow \infty$ , the average occupation asymptotically reaches an equilibrium stationary state where for each site, it becomes equal to the reservoir density  $\rho_a$ . For algebraic convenience, we write this as

$$\langle n_i(\tau) \rangle = \rho_a + \langle \delta n_i(\tau) \rangle \quad (\text{D.2})$$

such that the time dependent part follows a linear homogeneous equation

$$\frac{d \langle \delta n_i(\tau) \rangle}{d\tau} = \begin{cases} -(1 + \gamma) \langle \delta n_1(\tau) \rangle + \langle \delta n_2(\tau) \rangle & \text{for } i = 1 \\ \langle \delta n_{i-1}(\tau) \rangle - 2 \langle \delta n_i(\tau) \rangle + \langle \delta n_{i+1}(\tau) \rangle & \text{for } i \geq 2. \end{cases} \quad (\text{D.3})$$

The equation (D.3) is of form

$$\frac{d \langle \delta n(\tau) \rangle}{d\tau} = \mathcal{M} \langle \delta n(\tau) \rangle \quad (\text{D.4})$$

where the infinite matrix

$$\mathcal{M} = \begin{pmatrix} -(1 + \gamma) & 1 & 0 & 0 & \cdots \\ 1 & -2 & 1 & 0 & \cdots \\ 0 & 1 & -2 & 1 & \cdots \\ \vdots & \vdots & \vdots & \vdots & \ddots \end{pmatrix} \quad (\text{D.5})$$

The eigenvalues of this symmetric matrix  $\mathcal{M}$  are

$$\Lambda(\theta) = 2 \cos \theta - 2 \quad (\text{D.6})$$

for all  $0 \leq \theta < 2\pi$  and the associated eigenvector  $|\Psi(\theta)\rangle$  with components

$$\Psi_i(\theta) = \sqrt{2} \frac{\sin \theta i + (\gamma - 1) \sin \theta (i - 1)}{\sqrt{1 + (\gamma - 1)^2 + 2(\gamma - 1) \cos \theta}} \quad (\text{D.7})$$

for  $i = 1, 2, 3, \dots$ .

In the eigenvector basis, the solution of (D.3) is

$$\langle \delta n_i(\tau) \rangle = \int_0^{2\pi} \frac{d\theta}{2\pi} e^{\Lambda(\theta)\tau} \Psi_i(\theta) \sum_{j=1}^{\infty} \Psi_j(\theta) \langle \delta n_j(0) \rangle. \quad (\text{D.8})$$

In the hydrodynamic limit with  $\gamma = \frac{\Gamma}{\sqrt{T}}$  and for a large  $T$ , the solution  $\langle \delta n_i(\tau) \rangle \simeq \left\langle \delta \rho \left( \frac{i}{\sqrt{T}}, \frac{\tau}{T} \right) \right\rangle$  where

$$\langle \delta \rho(x, t) \rangle = 2 \int_0^{2\pi L} \frac{d\lambda}{2\pi} e^{-\lambda^2 t} \psi(x) \int_0^{\infty} dy \psi(y) \langle \delta \rho(y, 0) \rangle \quad (\text{D.9})$$

where

$$\psi(x) = \sin \lambda x + \frac{\lambda}{\Gamma} \cos \lambda x. \quad (\text{D.10})$$

It is straightforward to verify that the solution (D.9) satisfies the diffusion equation with the Robin boundary condition

$$\langle \delta \rho(x, t) \rangle - \frac{1}{\Gamma} \frac{\partial \langle \delta \rho(x, t) \rangle}{\partial x} = 0 \quad \text{at } x = 0. \quad (\text{D.11})$$

This shows that the average density  $\rho_{\text{av}}(x, t) = \rho_a + \langle \delta \rho(x, t) \rangle$  follows the hydrodynamic equation (10a, 10b).

**Remark:** For a uniform initial state  $\rho(x, 0) = \rho_b$ , the evolution of the average density is given in (42). At large times, the density at the boundary asymptotically approaches the reservoir density  $\rho_a$  as  $\rho_a + \frac{\rho_b - \rho_a}{\Gamma \sqrt{\pi t}}$ .

## Appendix E. Cumulants of the SSEP in slow coupling regime

For arbitrary boundary rates, we need to solve for the perturbation fields using the appropriate boundary conditions imposed on the respective fields at  $x = 0$  which are shown in (60a - 61b). The solution of the fields at the leading order in perturbation are

$$p_1(x, t) = \int_0^\infty dy g(x, y, 1 - t) \quad (\text{E.1})$$

and with  $q_1(x, t) = -\partial_x \psi_1(x, t)$

$$\begin{aligned} \psi_1(x, t) = & xC_1(t) + \int_0^\infty dy \tilde{g}(x, y, t) (\psi_1(y, 0) - yC_1(0)) \\ & + \int_0^t ds \int_0^\infty dy \tilde{g}(x, y, t - s) \left( \sigma(\rho_{\text{av}}(y, s)) \frac{\partial p_1(y, s)}{\partial y} - y \frac{dC_1(s)}{ds} \right) \end{aligned} \quad (\text{E.2})$$

where the expression of the first and the second Green's functions provided in (34) and (B.8) respectively and  $C_1(t)$  is defined in (60b).

Similarly, the solution of the fields at the second order in perturbation are

$$\begin{aligned} p_2(x, t) = & C_2(1 - t) - C_2(1) \int_0^\infty dy g(x, y, 1 - t) \\ & + \int_t^1 ds \int_0^\infty dy g(x, y, s - t) \left[ \frac{\sigma'(\rho_{\text{av}}(y, 1 - s))}{2} \left( \frac{\partial p_1(y, 1 - s)}{\partial y} \right)^2 \right. \\ & \left. + \frac{dC_2(1 - s)}{ds} \right] \end{aligned} \quad (\text{E.3})$$

and with  $q_2(x, t) = -\partial_x \psi_2(x, t)$

$$\begin{aligned} \psi_2(x, t) = & xC_3(t) + \int_0^\infty dy \tilde{g}(x, y, t) (\psi_2(y, 0) - yC_3(0)) \\ & + \int_0^t ds \int_0^\infty dy \tilde{g}(x, y, t - s) \left( q_1(y, s) \sigma'(\rho_{\text{av}}(y, s)) \frac{\partial p_1(y, s)}{\partial y} \right. \\ & \left. + \sigma(\rho_{\text{av}}(y, s)) \frac{\partial p_2(y, s)}{\partial y} - y \frac{dC_3(s)}{ds} \right) \end{aligned} \quad (\text{E.4})$$

with  $C_2(t)$  and  $C_3(t)$  defined in (61a) and (61b) respectively.

We can now use the above solutions of the perturbation fields in the formal expressions of the variance and the third cumulant given in (64-67).

## References

- [1] L. Bertini, A. De Sole, D. Gabrielli, G. Jona-Lasinio, C. Landim, Macroscopic fluctuation theory 87 (2) 593–636. doi:10.1103/RevModPhys.87.593.
- [2] B. Derrida, Microscopic versus macroscopic approaches to non-equilibrium systems 2011 (01) P01030. doi:10.1088/1742-5468/2011/01/P01030.
- [3] L. Bertini, A. De Sole, D. Gabrielli, G. Jona-Lasinio, C. Landim, Fluctuations in Stationary Nonequilibrium States of Irreversible Processes 87 (4) 040601. doi:10.1103/PhysRevLett.87.040601.
- [4] L. Bertini, A. De Sole, D. Gabrielli, G. Jona-Lasinio, C. Landim, Macroscopic Fluctuation Theory for Stationary Non-Equilibrium States 107 (3) 635–675. doi:10.1023/A:1014525911391.
- [5] B. Derrida, J. L. Lebowitz, E. R. Speer, Large Deviation of the Density Profile in the Steady State of the Open Symmetric Simple Exclusion Process 107 (3) 599–634. doi:10.1023/A:1014555927320.
- [6] T. Bodineau, B. Derrida, Current Fluctuations in Nonequilibrium Diffusive Systems: An Additivity Principle 92 (18) 180601. doi:10.1103/PhysRevLett.92.180601.
- [7] B. Derrida, B. Douçot, P. E. Roche, Current fluctuations in the one-dimensional symmetric exclusion process with open boundaries, Journal of Statistical Physics 115 (3-4) (2004) 717–748. doi:10.1023/b:joss.0000022379.95508.b2.
- [8] J. Tailleur, J. Kurchan, V. Lecomte, Mapping Nonequilibrium onto Equilibrium: The Macroscopic Fluctuations of Simple Transport Models 99 (15) 150602. doi:10.1103/PhysRevLett.99.150602.
- [9] L. Bertini, A. De Sole, D. Gabrielli, G. Jona-Lasinio, C. Landim, Current Fluctuations in Stochastic Lattice Gases 94 (3) 030601. doi:10.1103/PhysRevLett.94.030601.
- [10] V. Lecomte, A. Imparato, F. van Wijland, Current Fluctuations in Systems with Diffusive Dynamics, in and out of Equilibrium, Progress of Theoretical Physics Supplement 184 (SUPPL. 184) (2010) 276–289. arXiv:arXiv:0911.0564v1, doi:10.1143/PTPS.184.276.
- [11] B. Derrida, A. Gerschenfeld, Current Fluctuations of the One Dimensional Symmetric Simple Exclusion Process with Step Initial Condition, J. Stat. Phys. 136 (2009) 1.
- [12] K. Mallick, H. Moriya, T. Sasamoto, Phys. Rev. Lett. 129 (4) (2022) 040601. doi:https://doi.org/10.1103/PhysRevLett.129.040601.
- [13] B. Derrida, A. Gerschenfeld, Current Fluctuations in One Dimensional Diffusive Systems with a Step Initial Density Profile 137 (5) 978. doi:10.1007/s10955-009-9830-1.
- [14] L. Bertini, D. Gabrielli, J. L. Lebowitz, Large Deviations for a Stochastic Model of Heat Flow 121 (5) 843–885. doi:10.1007/s10955-005-5527-2.
- [15] P. L. Krapivsky, K. Mallick, T. Sadhu, Large Deviations in Single-File Diffusion, Phys. Rev. Lett. 113 (7) (2014) 78101.
- [16] P. L. Krapivsky, K. Mallick, T. Sadhu, Tagged Particle in Single-File Diffusion, Journal of Statistical Physics 160 (4) (2015) 885–925. doi:10.1007/s10955-015-1291-0.
- [17] A. Krajenbrink, P. Le Doussal, Inverse scattering of the zakharov-shabat system solves the weak noise theory of the kardar-parisi-zhang equation, Phys. Rev. Lett. 127 (2021) 064101. doi:10.1103/PhysRevLett.127.064101.
- [18] B. Meerson, E. Katzav, A. Vilenkin, Large Deviations of Surface Height in the Kardar-Parisi-Zhang Equation, Physical Review Letters 116 (7) (2016) 070601. doi:10.1103/PhysRevLett.116.070601.

- [19] T. M. Liggett, Ergodic theorems for the asymmetric simple exclusion process, *Transactions of the American Mathematical Society* 213 (1975) 237–261.
- [20] S. Grosskinsky, Phase transitions in nonequilibrium stochastic particle systems with local conservation laws, Ph.D. thesis, Technical University of Munich (2004).
- [21] L. Williams, T. Sasamoto, *Combinatorics of the Asymmetric Exclusion* (2000). [arXiv:1204.1114v1](#).
- [22] H. G. Duhart, P. Mörters, J. Zimmer, The Semi-infinite Asymmetric Exclusion Process: Large Deviations via Matrix Products, *Potential Analysis* 48 (3) (2018) 301–323. [doi:10.1007/s11118-017-9635-9](#).
- [23] C. A. Tracy, H. Widom, The asymmetric simple exclusion process with an open boundary, *Journal of Mathematical Physics* 54 (10) (2013). [doi:10.1063/1.4822418](#).
- [24] P. L. Krapivsky, Symmetric exclusion process with a localized source, *Physical Review E - Statistical, Nonlinear, and Soft Matter Physics* 86 (4) (2012) 1–7. [doi:10.1103/PhysRevE.86.041103](#).
- [25] B. Derrida, O. Hirschberg, T. Sadhu, Large Deviations in the Symmetric Simple Exclusion Process with Slow Boundaries, *Journal of Statistical Physics* 182 (1) (2021) 15. [doi:10.1007/s10955-020-02680-3](#).
- [26] R. Baldasso, O. Menezes, A. Neumann, R. R. Souza, Exclusion Process with Slow Boundary, *Journal of Statistical Physics* 167 (5) (2017) 1112–1142. [doi:10.1007/s10955-017-1763-5](#).
- [27] T. Franco, P. Gonçalves, A. Neumann, Non-equilibrium and stationary fluctuations of a slowed boundary symmetric exclusion, *Stochastic Processes and their Applications* 129 (4) (2019) 1413–1442. [arXiv:1608.04317](#), [doi:10.1016/j.spa.2018.05.005](#).
- [28] T. Franco, P. Gonçalves, A. Neumann, Equilibrium fluctuations for the slow boundary exclusion process, in: *Springer Proceedings in Mathematics and Statistics*, Vol. 209, 2017, pp. 177–197. [arXiv:1612.01004](#), [doi:10.1007/978-3-319-66839-0\\_9](#).
- [29] P. Gonçalves, M. Jara, O. Menezes, A. Neumann, Non-equilibrium and stationary fluctuations for the SSEP with slow boundary, *Stochastic Processes and their Applications* 130 (7) (2020) 4326–4357. [arXiv:1810.05015](#), [doi:10.1016/j.spa.2019.12.006](#).
- [30] K. Tsunoda, Hydrostatic limit for exclusion process with slow boundary revisited, *ArXiv e-prints* 1902.06210 (feb 2019). [arXiv:1902.06210](#).
- [31] C. Franceschini, P. Gonçalves, B. Salvador, Hydrodynamical behavior for the generalized symmetric exclusion with open boundary. [arXiv:2201.10241](#), [doi:10.48550/arXiv.2201.10241](#).
- [32] C. Franceschini, P. Gonçalves, F. Sau, Symmetric inclusion process with slow boundary: Hydrodynamics and hydrostatics. [arXiv:2007.11998](#), [doi:10.48550/arXiv.2007.11998](#).
- [33] B. Derrida, O. Hirschberg, T. Sadhu, Large Deviations in the Symmetric Simple Exclusion Process with Slow Boundaries, *Journal of Statistical Physics* 182 (1) (2021) 15. [doi:10.1007/s10955-020-02680-3](#).
- [34] T. Bodineau, M. Lagouge, Current Large Deviations in a Driven Dissipative Model, *Journal of Statistical Physics* 139 (2) (2010) 201–218. [arXiv:0910.0426](#), [doi:10.1007/s10955-010-9934-7](#).
- [35] A. De Masi, E. Presutti, D. Tsagkarogiannis, M. E. Vares, Current Reservoirs in the Simple Exclusion Process, *Journal of Statistical Physics* 144 (6) (2011) 1151–1170. [doi:10.1007/s10955-011-0326-4](#).
- [36] A. De Masi, E. Presutti, D. Tsagkarogiannis, M. E. Vares, Non-equilibrium Stationary States in the Symmetric Simple Exclusion with Births and Deaths, *Journal of Statistical Physics* 147 (3) (2012) 519–528. [doi:10.1007/s10955-012-0481-2](#).
- [37] T. Franco, P. Gonçalves, A. Neumann, Hydrodynamical behavior of symmetric exclusion with slow bonds, *Annales de l’Institut Henri Poincaré, Probabilités et Statistiques* 49 (2) (2013) 402–427. [doi:10.1214/11-AIHP445](#).
- [38] F. Redig, K. Vafayi, Weak coupling limits in a stochastic model of heat conduction, *Journal of*

- Mathematical Physics 52 (9) (2011) 093303. [arXiv:1101.2877](#), [doi:10.1063/1.3638042](#).
- [39] C. Landim, K. Tsunoda, Hydrostatics and dynamical large deviations for a reaction-diffusion model, *Annales de l'Institut Henri Poincaré, Probabilités et Statistiques* 54 (1) (2018) 51–74. [doi:10.1214/16-AIHP794](#).
- [40] C. Erignoux, P. Gonçalves, G. Nahum, Hydrodynamics for SSEP with non-reversible slow boundary dynamics: Part I, the critical regime and beyond, *ArXiv e-prints* 1912.09841 (dec 2019). [arXiv:1912.09841](#).
- [41] J. Tailleur, J. Kurchan, V. Lecomte, Mapping out-of-equilibrium into equilibrium in one-dimensional transport models 41 (50) 505001. [doi:10.1088/1751-8113/41/50/505001](#).
- [42] P. Martin, E. Siggia, H. Rose, Statistical Dynamics of Classical Systems, *Physical Review A* 8 (1) (1973) 423–437. [doi:10.1103/PhysRevA.8.423](#).
- [43] C. De Dominicis, L. Peliti, Field-theory renormalization and critical dynamics above  $T_c$ : Helium, antiferromagnets, and liquid-gas systems, *Phys. Rev. B* 18 (1978) 353–376. [doi:10.1103/PhysRevB.18.353](#).
- [44] B. Derrida, Non-equilibrium steady states: Fluctuations and large deviations of the density and of the current 2007 (07) P07023–P07023. [doi:10.1088/1742-5468/2007/07/P07023](#).
- [45] T. Sadhu, B. Derrida, Large deviation function of a tracer position in single file diffusion 2015 (9) P09008. [doi:10.1088/1742-5468/2015/09/P09008](#).
- [46] P. L. Krapivsky, B. Meerson, Fluctuations of current in nonstationary diffusive lattice gases 86 (3) 031106. [doi:10.1103/PhysRevE.86.031106](#).
- [47] P. L. Krapivsky, K. Mallick, T. Sadhu, Melting of an Ising quadrant, *Journal of Physics A: Mathematical and Theoretical* 48 (1) (2015) 015005. [doi:10.1088/1751-8113/48/1/015005](#).
- [48] P. L. Krapivsky, K. Mallick, T. Sadhu, Tagged Particle in Single-File Diffusion 160 (4) 885–925. [doi:10.1007/s10955-015-1291-0](#).
- [49] E. Bettelheim, N. R. Smith, B. Meerson, Full statistics of nonstationary heat transfer in the kipnis–marchioro–presutti model, *Journal of Statistical Mechanics: Theory and Experiment* 2022 (9) (2022) 093103. [doi:10.1088/1742-5468/ac8a4d](#).
- [50] A. Lefèvre, G. Biroli, Dynamics of interacting particle systems: Stochastic process and field theory, *Journal of Statistical Mechanics: Theory and Experiment* 2007 (7) (2007) P07024–P07024. [arXiv:0709.1325](#), [doi:10.1088/1742-5468/2007/07/P07024](#).